

Probabilistic multiscale analysis of inelastic localized failure in solid mechanics

Adnan Ibrahimbegovic, Hermann G. Matthies

Ecole Normale Supérieure, Cachan, France

TU Braunschweig, Germany

e-mail: ai@lmt.ens-cachan.fr, wire@tu-bs.de

In this work, we discuss the role of probability in providing the most appropriate multiscale based uncertainty quantification for the inelastic nonlinear response of heterogeneous materials undergoing localized failure. Two alternative approaches are discussed: i) the uncertainty quantification in terms of constructing the localized failure models with random field as parameters of failure criterion, ii) the uncertainty quantification in terms of the corresponding Bayesian updates of the corresponding evolution equation. The detailed developments are presented for the model problem of cement-based composites, with a two-phase meso-scale representation of material microstructure, where the uncertainty stems from the random geometric arrangement of each phase. Several main ingredients of the proposed approaches are discussed in detail, including microstructure approximation with a structured mesh, random field KLE representation, and Bayesian update construction. We show that the first approach is more suitable for the general case where the loading program is not known and the best one could do is to quantify the randomness of the general failure criteria, whereas the second approach is more suitable for the case where the loading program is prescribed and one can quantify the corresponding deviations. More importantly, we also show that models of this kind can provide a more realistic prediction of localized failure phenomena including the probability based interpretation of the size effect, with failure states placed anywhere in-between the two classical bounds defined by continuum damage mechanics and linear fracture mechanics.

Keywords: multiscale analysis, inelastic behavior, uncertainty quantification, fracture, size-effect.

1. INTRODUCTION AND MOTIVATION

In this paper, we address several important issues related to the numerical analysis of quasi-brittle failure processes, chief among them is how to account for heterogeneities of real materials and how to transfer the appropriate information provided from fine scales. Most case studies and detailed illustration of ideas pertaining to heterogeneities and related uncertainties are given for cement-based composite materials, such as concrete or mortar, certainly the most widely used man-made materials. The mechanical behavior of heterogeneous materials can be represented at different scales, depending upon the objectives and the physical mechanisms that are important to account for. The choice of scale is also closely related to the corresponding uncertainty description.

Given computational resources for typical engineering applications, most frequently we ought to perform an analysis at the structure scale or macro-scale. At these scales, cement-based materials might be considered as homogeneous, and their properties obtained by using the key concept of Representative Volume Element (RVE, see [7, 30]) to retrieve phenomenological models of inelastic behavior (e.g. see [2, 21, 77]). Those models are well known for their robustness and lead to a relatively moderate computational cost. Due to these two main points, phenomenological approaches are widely used. On the other hand, such models are based on a set of “material” parameters which need to be identified (e.g., see [32, 35]), mainly from experiments providing unique load paths and boundary conditions. Hence, this “natural” methodology leads to a set of parameters which is

linked to the chosen load-path. As they are not adapted to another path, it is difficult to get any predictive features from those phenomenological macro-models. The main reason for this is that the macro-scale is not the right scale to consider with the aim to model failure of heterogeneous materials. Many authors tried to overcome this major drawback by furnishing micro-mechanical bases to the macroscopic model set of parameters (see [37, 42, 79]) and provide more predictive macro-scale models. One possible way to achieve such a goal is to adopt homogenization methods which lead to accurate results for linear problems. In the presence of non-linearities such methods are not capable to provide good estimates for the effective (macroscopic) properties (see [16]). Moreover, such an approach does not take into account the inherent uncertainties attached to heterogeneous materials and structures.

At a finer scale than the macroscopic one, cement-based materials appear to be heterogeneous exhibiting an important variability. This variability might be viewed from the geometrical point of view, considering the arrangement (positions, shapes) of the different phases. In this work, we propose to take account of the meso-scale variability in order to compute the macroscopic (effective) properties' statistics for a porous medium made of a non-linear matrix. Moreover, we show how these statistics (mainly the correlation length through the covariance function) might be used at the macroscopic level to model particular features of cement-based materials such as size effects. The key point is that the material parameters at the meso-scale are assumed to be deterministic, so that the variability is only related to the size and the positions of the voids in the porous media. In order to solve this stochastic problem and compute the statistical moments for the response quantities, we employ the Monte-Carlo method within a distributed software environment. This stochastic integration method is based on many evaluations of the meso-structural response, thus leading to a time-consuming process. Moreover, as the error can directly be evaluated in terms of the number of realizations, it is necessary to choose a relatively small discrete problem, even in the case of complex meso-structures. To achieve this we propose a model based on a regular mesh which is not constrained by the physical interfaces. This model relies on either finite element or discrete element representation of material microstructure, whose kinematic description is enriched by the use of strain and displacements discontinuities in order to represent two phases.

The first approach we propose is referred to as sequential, where the results obtained at the fine scale are used to define the probabilistic variation of the phenomenological model parameters used at the macro scale. The key advantage of the sequential approach is to provide the appropriate probabilistic description in agreement with the given material microstructure.

Another very important advantage of the sequential model is its ability to provide a sound explanation of the size effect encountered in failure phenomena of engineering structures built from quasi-brittle materials. The approach to failure analysis we propose is placed within a stochastic framework, which provides a very good basis for taking into account the intrinsic randomness of the heterogeneities of real building materials: concrete, mortar, soils or any other geo-material. Such materials have a particular mechanical behavior, known as quasi-brittle, which can be seen as a subcategory of softening materials (see [21]). A typical failure pattern we should be able to represent contains the fracture process zone (FPZ) along with the macro-crack that is a final threat for the structural integrity (see Fig. 1a). In the context of a simple 1D model interpretation, this behavior can be described with four material parameters (e.g., see [22] or [9]): Young's modulus E , the yield stress σ_y which induces micro-cracking or the FPZ creation, and the failure stress σ_u which induces macro-cracking after the sudden coalescence of the micro-cracks leading to a softening behavior (see Fig. 1b). The last parameter is the fracture energy G_f [J.m^{-2}], which represents the amount of energy necessary to create and open a macro-crack.

Several theories exist on how to model failure in quasi-brittle materials, and most of them link the micro-cracks coalescence phenomenon to a size effect, a dependency on the size of a structure to its failure load. The aim of all those theories is to combine continuum damage mechanics (CDM), where the failure stress does not depend on the size of the structure, to linear fracture mechanics (LFM), where a size effect appears naturally as the logarithm of the failure stress depends linearly

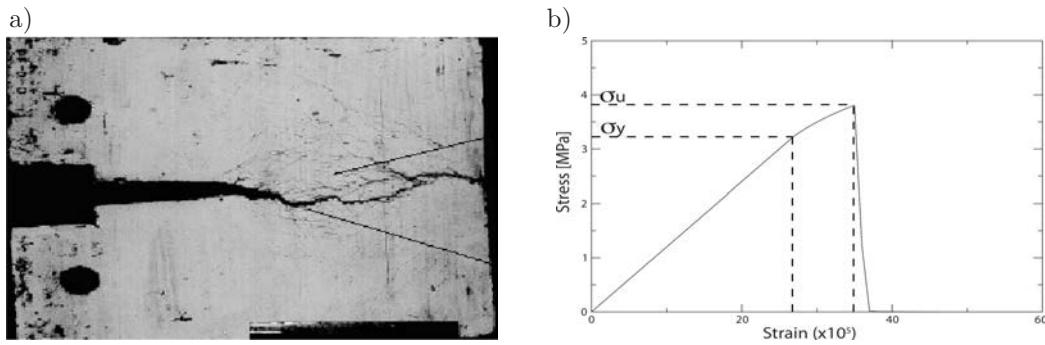


Fig. 1. Tensile test behavior: a) typical quasi-brittle failure pattern in engineering structure, b) quasi-brittle material 1D model.

on the logarithm of the size of the structure (see Fig. 16). It can be experimentally demonstrated that even if purely brittle materials follow LFM, quasi-brittle materials do not, and instead they follow a non-linear relationship between the two previous logarithms of the failure stress and the size of the structure. These materials exhibit a different size effect than the one encountered for purely brittle materials.

The second approach we propose is the simultaneous, where the response of the meso-structure can not be precomputed as in the sequential approach. Here the interaction between macro- and meso-scale is considered so strong that it is not possible, or rather not meaningful, to try and precompute all possible response. This may happen in regions where severe irreversible material processes occur, such that the deformation path of the macro-scale, which is imposed onto the meso-scale, influences the meso-scale response in some profound way. Our idea is that this approach can actually be combined with the sequential approach described previously. The sequential approach is regarded as the “standard” way of transferring the meso-scale properties to the macro-scale. But in the circumstances just alluded to – severe meso-scale material irreversibility – the simultaneous approach could be switched on like a magnifying “zoom lens”, and the meso-scale simulation can run simultaneously coupled with the macro-scale computation. The response at the meso-scale can then be used not to just identify the properties of macro-scale phenomenological models, but the macro-scale state of the system itself. The state of the macro-scale is updated through a Bayesian procedure directly from the meso-scale.

Both on the meso-scale level as well as on the macro-scale level, we see that mechanical models with a probabilistic description have to be dealt with both in a modelling aspect as well as numerically. As described here, on the meso-scale only ‘geometric’ uncertainties are considered – although material uncertainties could easily be added – whereas on the macro-scale the continuum mechanics material description is probabilistic. For more details and a general overview of these general modelling and numerical aspects, see, e.g., [46, 47].

The outline of this paper is as follows: Sec. 2 is devoted to the description of the sequential approach; in Subsec. 2.1 we present the ingredients along with a detailed illustration for a meso-scale level description, with the plasticity model employed and the structured mesh representation, leading to a fast computation of non-linear response without any remeshing. In Subsec. 2.2 we describe the stochastic problem, the geometrical description process for defining the meso-structure and the stochastic integration method. The following Subsec. 2.3 describes the probabilistic characterisation of the material on the macro-scale. Subsection 2.4 presents the results obtained for the SRVE size, as well as the corresponding macroscopic properties statistics. Finally, Subsec. 2.5 deals with size effect modelling based on second order correlated macroscopic material property fields. In Sec. 3 we present the details of the simultaneous approach. Many items are analogous as in the sequential approach and thus can be mentioned only briefly. What is described in more detail is the identification process for the macro-state from the meso-scale response. Concluding remarks are given in Sec. 4.

2. SEQUENTIAL APPROACH FOR PROBABILISTIC MULTISCALE ANALYSIS

2.1. Meso-scale model of material heterogeneities with deterministic material parameters

Meshing is one of the major issues in modelling heterogeneous materials. The possibly high number of phases and their complex shapes frequently might lead to a quite high number of degrees-of-freedom and also quite distorted meshes. Moreover, the meshing process itself might consist in a complex and time-consuming algorithm. The objective of this first part is to show how to employ structured meshes in order to simplify the meshing process of heterogeneous materials. Hence, this section presents the main ideas leading to regular meshes which are not constraint by the physical interfaces between the different phases. The key ingredients to provide such models are field discontinuities introduced inside the elements in which the physical interfaces are present. These kinematics enhancements might be developed within the framework of the incompatible modes method (see [25, 74]), and require a dedicated solution algorithm which is illustrated next.

2.1.1. Structured mesh and element kinematics enhancements

At the meso-scale, we consider a heterogeneous material in 2D built of different phases and we assume that each of these phases is described by the inclusions positions and shapes. In order to model such material with a structured mesh, Fig. 2 shows a typical 3-nodes triangular finite element representing two phases. Those two phases are introduced through two types of discontinuities (see [24]), namely a discontinuity of the strain field and a discontinuity of the displacement field, both of them lying at the same position (prescribed by the known physical interface between the two phases). The strain discontinuity permits the proper strain representation of two different sets of elastic properties corresponding to each phase. The displacement discontinuity leads to the possibility to model debonding or any failure mechanism at the interface. For the latter, two failure mechanisms are considered: one corresponding to the opening of the crack in the normal direction and the second one to the sliding in the tangent direction (see [66]). Both of these discontinuities are introduced by using the incompatible modes method (see [25, 74]). The key advantage of this method is to lead to a constant number of global degrees-of-freedom.

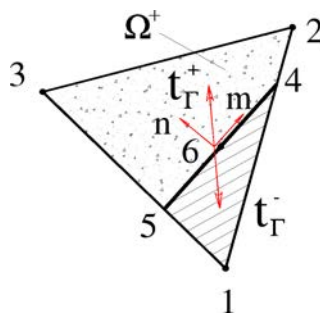


Fig. 2. Two phase 3-node triangular element, interface position and the corresponding sub-domains.

Both of those kinematics enhancements are added on top of the standard CST element (Fig. 2). Hence, this element is divided into two parts by introducing an interface whose position is obtained by the intersection of the chosen structured mesh with the inclusions placed within the structure. The domain Ω^e of the standard 3-node constant stress triangle (CST) element is thus divided into two sub-domains Ω^{e^-} and Ω^{e^+} . One of the most important and well-known features of strong (displacement field) discontinuity models is their capability to be independent from the mesh, even for softening laws. This ability is based in the fact that the dissipation process occurs on a line (i.e., the interface) and not in the whole volume. However, different elastic-plastic or elastic-damage

behavior laws, with positive hardening, might be chosen for each of the two sub-domains split by the interface, with different elastic properties (see [23]).

It is worth to note that the strain field discontinuity is always present, due to the different elastic constants between the two phases. In contrast and because of representing a failure mechanism between the two phases, the displacement field discontinuity needs to be activated according to some chosen failure criterion.

Introducing those discontinuities requires enhancement the kinematics of the element by using two incompatible modes. Thus, the displacement field might be written as follows:

$$\mathbf{u}^h(\underline{x}, t) = \sum_{a=1}^3 N_a(\underline{x}) \mathbf{d}_a(t) + \mathbf{M}_{\mathbf{I}}^\alpha(\underline{x}) \alpha_{\mathbf{I}}(t) + \mathbf{M}_{\mathbf{I}}^\beta(\underline{x}) \beta_{\mathbf{I}}(t) + \mathbf{M}_{\mathbf{II}}(\underline{x}) \alpha_{\mathbf{II}}(t). \quad (1)$$

This expression contains four terms: the first one provides a constant strain field inside the element (as the classical CST element does). The second and third terms both represent jumps in the displacements field, in the normal and the tangential directions. Finally, the last part provides the strain field discontinuity. All the strain and displacement enhancements are limited to a single element only; the latter provides a much better basis for constructing robust operator split analysis from the X-FEM method. The shape functions $\mathbf{M}_{\mathbf{I}}(\underline{x})$ for the first incompatible mode (see Fig. 3a.) corresponding to the displacements field discontinuity for both normal and tangent directions (see [22]) might be written as:

$$\mathbf{M}_{\mathbf{I}}(\underline{x}) = H_{\Gamma_s}(\underline{x}) - \sum_{a \in \Omega^+} N_a(\underline{x}), \quad (2)$$

where N_a represents the normal CST shape functions element and H_{Γ_s} the Heaviside function placed at the interface position. The shape function $\mathbf{M}_{\mathbf{II}}(\underline{x})$ which provides the jump in the strain field is shown on Fig. 3b.

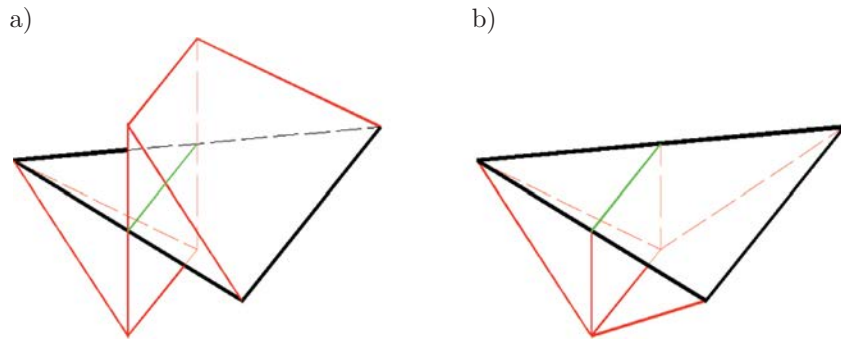


Fig. 3. Incompatible modes corresponding to displacements a) and strain b) discontinuities for the CST element.

Considering the displacement interpolation (1), the strain field might be written as

$$\varepsilon^h(\underline{x}, t) = \mathbf{B} \mathbf{d} + \mathbf{G}_{\mathbf{II}} \alpha_{\mathbf{II}} + (\mathbf{n}^T \otimes \mathbf{n}) \mathbf{G}_{\mathbf{I}_r}^\alpha \alpha_{\mathbf{I}} + \frac{1}{2} [\mathbf{n}^T \otimes \mathbf{m} + \mathbf{m}^T \otimes \mathbf{n}] \mathbf{G}_{\mathbf{I}_r}^\beta \beta_{\mathbf{I}}, \quad (3)$$

where $\mathbf{B}(\underline{x})$ are the well-known CST element strain-displacement matrixes (e.g., see [77]) and $\mathbf{G}_{\mathbf{I}_r}(\underline{x})$ contains the derivatives of the first incompatible mode. Finally, in (4), $\mathbf{G}_{\mathbf{II}}$ is the matrix containing the derivatives of the second shape function $\mathbf{M}_{\mathbf{II}}(\underline{x})$.

2.1.2. Operator split solution procedure for computing interface failure modes

Deriving from the incompatible modes method for the two kind of discontinuities added on the top of the classical CST element (strain field and displacement field), the total system to be solved

consists of four equilibrium equations, with (4a) as the global equilibrium equation and (4b) to (4d) are corresponding to the local ones. It is worth to remind that Eqs. (4b) and (4c) have to be solved only in case of activation of the displacement discontinuity in the normal or the tangent direction.

$$\left\{ \begin{array}{l} A_{e=1}^{nel} [f^{int} - f^{ext} = 0] \\ \mathbf{h}_I^{\alpha,e} = 0 \\ \mathbf{h}_I^{\beta,e} = 0 \\ \mathbf{h}_{II}^e = 0 \end{array} \right. \Rightarrow \left\{ \begin{array}{l} \int_{\Omega^e} \mathbf{B}^T \sigma d\Omega - \int_{\Omega^e} \mathbf{N}^T b d\Omega = 0, \\ \int_{\Omega^e} \mathbf{G}_{I_v}^{\alpha,T} \sigma d\Omega = 0, \\ \int_{\Omega^e} \mathbf{G}_{I_v}^{\beta,T} \sigma d\Omega = 0, \\ \int_{\Omega^e} \mathbf{G}_{II}^T \sigma d\Omega = 0. \end{array} \right. \quad (4)$$

The consistent linearization (e.g., see [21]) of this set of equations leads to a linear system, in matrix form:

$$\left[\begin{array}{cccc} \mathbf{K}^e & \mathbf{F}_{I_r}^{\alpha,e} & \mathbf{F}_{I_r}^{\beta,e} & \mathbf{F}_{II}^e \\ \mathbf{F}_{I_r}^{\alpha,eT} & \mathbf{H}_I^{\alpha,e} & \mathbf{F}_H^e & \mathbf{F}_S^{\alpha,e} \\ \mathbf{F}_{I_r}^{\beta,eT} & \mathbf{F}_H^{eT} & \mathbf{H}_I^{\beta,e} & \mathbf{F}_S^{\beta,e} \\ \mathbf{F}_{II}^{e,T} & \mathbf{F}_S^{\alpha,eT} & \mathbf{F}_S^{\beta,eT} & \mathbf{H}_{II}^e \end{array} \right]_{n+1}^{(k)} \begin{pmatrix} \Delta d \\ \Delta \alpha_I \\ \Delta \beta_I \\ \Delta \alpha_{II} \end{pmatrix}_{n+1}^{(k+1)} = \begin{pmatrix} -r \\ -\mathbf{h}_I^{\alpha,e} \\ -\mathbf{h}_I^{\beta,e} \\ -\mathbf{h}_{II}^e \end{pmatrix}_{n+1}^{(k)}. \quad (5)$$

The expanded form for each block can be found in [17].

The operator split strategy consists in first solving the local equations of system (4) (namely Eqs. (4b) to (4d)) at each numerical integration point and for fixed global degrees-of-freedom values. The second step is then to carry out a static condensations (e.g., see [75]). These static condensations leads to the effective stiffness matrix (see [67] and [17] and thus the last step is to solve the global system of Eq. (4) to obtain the updated value of the displacement field $d_{n+1}^{(k+1)} = d_{n+1}^{(k)} + \Delta d_{n+1}^{(k+1)}$ from

$$\widehat{\mathbf{K}}_{n+1}^{(k)} \cdot \Delta d_{n+1}^{(k+1)} = -r_{n+1}^{(k)}. \quad (6)$$

One of the key points to note is that the total number of global unknowns remains the same as with the standard CST element which is a major advantage of the ‘incompatible modes method’. Simple illustrative examples dealing with the use of structured meshes might be found in [17].

2.1.3. Comparison between structured and unstructured mesh computations

Here, we aim to make a comparison between structured and unstructured meshes in order to assess the capability for both cases to get very close results. For this we consider a porous material made of a perfectly plastic matrix with circular voids of different sizes. The first case (Fig. 4a) presents an exact mesh obtained by using the software GMSH. Obviously, in this case each element contains only one phase (namely the matrix or the “voids”). Moreover, several elements are strongly distorted and they exhibit quite different sizes. For these two reasons the stiffness matrix is poorly conditioned. The second case (Fig. 4b) relies on a structured mesh which is based on a regular grid. In this case, the elements need to represent two phases to model the inclusions and we adopt the strategy presented at the beginning of this Section. Figure 4 shows the axial displacement contour plot (with an amplification factor of 100) for both unstructured and structured meshes. Figure 5 plots the corresponding macroscopic axial reactions displacement curve.

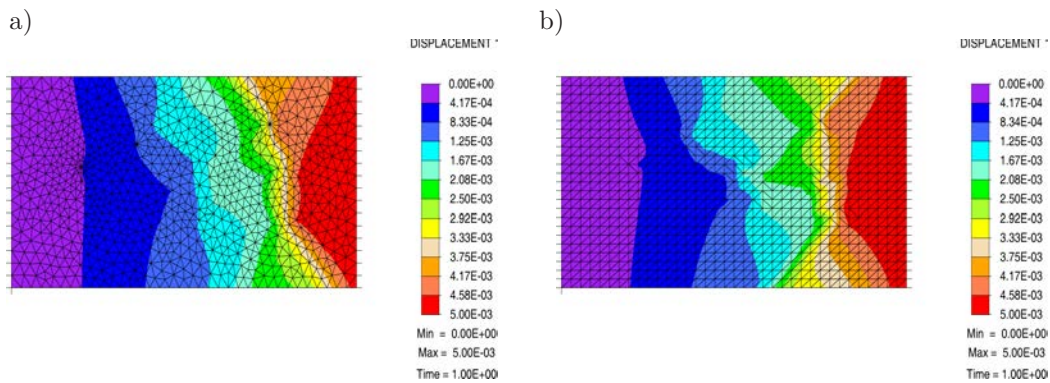


Fig. 4. Longitudinal displacement contour plot corresponding to max.load a) for adaptive mesh and b) regular mesh.

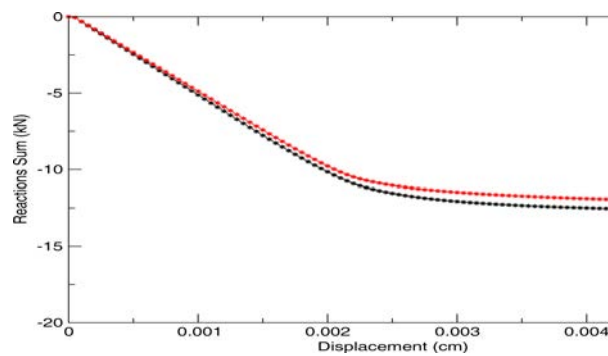


Fig. 5. Reactions sum vs. displacement curve (black unstructured mesh, red structured mesh).

We show that both cases are providing very close results, but with a gain of computing time in favor of the structured mesh strategy (this point is mainly due to the tangent matrix optimal conditioning). Combined to a meshing process which is much easier, the structured mesh way appears to be a good and accurate method to model heterogeneous materials, especially in the context of many realizations that have to be analyzed. This last point is one of the key issues considering probabilistic aspects for heterogeneous materials.

2.2. Probability aspects of inelastic localized failure for heterogeneous materials

At a finer scale than the macroscopic one, cement-based materials obviously appear to be heterogeneous. As an example, at this meso-scale mortars are made of three phases: two solid ones (the grains and the cement paste) and voids. It is well-known from experimental data that macroscopic properties of such materials are strongly linked to the (at least) meso-scale constituents. In [76], the authors gathered some experimental results showing the very important decrease of macroscopic mechanical strength (in tension or compression) along the increasing void volume fraction. Moreover, considering a constant porosity, the voids shapes and positions also have a major influence on the macroscopic properties, especially for small specimens. This key point is linked to the statistical RVE size (see e.g., [30]), which has to be determined along a prescribed macroscopic error tolerance. The main objective of this section is then to illustrate the possibilities provided by the use of a structured mesh representation and the efficient computational capabilities of the proposed model for dealing with random heterogeneities. To that end, we consider herein a porous material, typical of mortars at the meso-scale level. At this scale, we assume that such a material is characterized by a two-phase micro-structure with a solid phase and a fluid phase. The former will be referred as the “matrix” and the latter is supposed to represent the voids or inclusions. Depending on the

number of inclusions, their sizes and positions, the non-linear macroscopic response of such a material will vary. In other words, the macroscopic properties, such as Young's modulus or the yield stress, will be influenced by the meso-scale geometry. Our goals here are: first, to determine the statistical RVE size corresponding to such a geometry (morphological RVE); second, to carry out numerically the variations of the macroscopic characteristics upon the inclusion sizes and positions. The key point for this study is that the variability introduced into the model is restricted to the specimen geometry only, whereas the mechanical characteristics of the two phases are assumed to be deterministic. To be more precise, the matrix phase is supposed to be accurately modelled by an elastic-perfectly plastic model based upon the Drucker-Prager criterion (see [12]). The voids are represented by a simple linear isotropic elasticity model with very small Young's modulus value. In the following sections, we first begin to describe the Gibbs point process, leading to the realizations of the meso-structures. We also show an example of one typical mesh obtained and the corresponding macroscopic response to a tension test. Then, we turn to the stochastic integration method which has been chosen to numerically solve this problem and the corresponding software engineering aspects. Finally we present the methodology leading to the RVE definition and we discuss the results obtained for this stochastic problem.

2.2.1. Geometry description of material meso-structure

Here, we describe both the process and the hypothesis leading to the meshing procedure within a rectangular domain ($3.6 \times 1.8 \text{ cm}^2$). The meso-structure geometry of such a domain is here supposed to be accurately modelled by a Gibbs point process. Such a point process is built on a two steps scheme. The first one is the determination of the number of inclusions according to a Poisson's law. The second step consists in the determination of the inclusion center coordinates as well as of the radius for each inclusion. While such a Gibbs process already naturally leads to a set of non-intersecting inclusions, we applied an even more restrictive criterion, by choosing the minimal distance between the inclusions (here equal to 2 mm). Moreover, in order to be consistent with the mesh size and the model features, the inclusions' radii are bounded between 1 mm and 3 mm. Figure 6 shows a particular realization of the meso-structure and the corresponding structured mesh. We can notice that each inclusion is correctly modelled by a set of discontinuities without any major distortion.

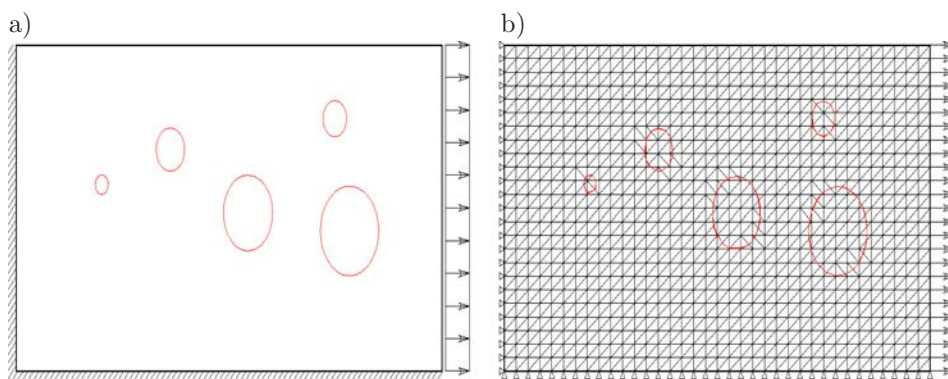


Fig. 6. a) Meso-structure geometry and b) corresponding structured mesh.

Since the material parameters are chosen to be deterministic, the statistics of the macroscopic response depend on the meso-structure geometry only, defined by the void volume fraction and consequently the voids' radii and center positions. Thus, the macroscopic problem is stochastic and requires a stochastic integration method which is presented in the next section.

2.2.2. Computation of stochastic integrals

As we just mentioned, the positions and sizes of the voids in the matrix are described by a discrete random field, based on a Gibbs point process. In a general sense, a 2D random point process might be viewed as a finite set of random variables, which are indexed by the vectors of spatial coordinates in R^2 . Thus the meso-structure geometry is defined as a random field, which implies that every solution computed by the mechanical model is also a random field (e.g., the structure displacement at a fixed point is a random variable). In this study, we are interested in characterizing the macroscopic mechanical properties of our structure. To achieve this goal, we use a global approach which consists in identifying the material properties governing the global behavior of the structure. More precisely, we aim to determine the effective global material properties by the corresponding identification of the global response computed by the finite element model. Therefore, since the global responses (displacement and reactions) are random variables, the global material properties we aim to identify, such as the Young's modulus or the yield stress, are also random variables.

A probabilistic characterization of the macroscopic mechanical properties can be viewed as describing the probabilistic law followed by each of these properties. Two approaches can be drawn to find a probabilistic law describing a random phenomena. The first one, the so-called frequentist approach [31], is based on statistical tests, like the χ^2 test for the Gaussian probability law. Results of these tests are error margins that evaluate how the outcomes of the given random phenomena fit with respect to a given probability law. The second, so-called Bayesian approach [26], is trying to use all the available information along with the maximum entropy theory (see [65, 69]) in order to provide the most general probability law for a given state of information; thus, to fully describe this probability law, the statistical moments of different orders have to be computed. In this work, the second approach is chosen. The macroscopic material properties we tend to characterize are all defined on the positive real line. Moreover, we assume that they can be given a mean value and a finite standard deviation. On the basis of such information, the maximum entropy theory leads to the most general probability law for this case in terms of the log-normal distribution, which is fully described by its computed mean value and standard deviation.

Consequently, in order to characterize the macroscopic mechanical properties using the Bayesian approach, the first two statistical moments of each of these properties have to be computed. The statistical moment of any random variable is an integral of a functional of this random variable over a probability space. Hence, an efficient numerical tool to compute such an integral in a multi-dimensional space is required. Rather than high order quadrature rules like the Smolyak algorithm [68], we use here a simple direct integration algorithm which is Monte Carlo simulation [8]. The basic idea of Monte Carlo simulation is to approximate the integrals of a functional of a random variable by a weighted sum of realizations of this random functional. Let ξ be a random variable defined on some probability space (Ω, B, P) , where Ω is the space of elementary events, B is a σ -algebra built on Ω , and P is a probability measure. Any defined function of ξ can be written as $\int_{\Omega} f(\xi(\omega))dP(\omega)$. The simple Monte Carlo algorithm consist in approximating this integral as a finite weighted sum of realizations $f(\xi(\omega_i))$, each computed at a randomly independently chosen point $\omega_i \in \Omega$, multiplied by the corresponding weight $\frac{1}{N}$ (with N the given number of realizations)

$$\int_{\Omega} f(\xi(\omega))dP(\omega) \approx \frac{1}{N} \sum_{i=1}^N f(\xi(\omega_i)). \quad (7)$$

For this kind of numerical integration, the convergence rate can be *a priori* estimated thanks to the central limit theorem [40]. It is found that the standard deviation of the error is proportional to the standard deviation of $f(\xi)$ over \sqrt{N} , N being the number of evaluations of $f(\xi)$. As each realization of the Gibbs process is stochastically independent from the others, this method can be directly applied here, and further more the computations may be easily parallelized using an

appropriate software environment to eliminate the main drawback of the Monte Carlo algorithm, the slow rate convergence. In this case, where no correlation exists in the geometrical space, other tools such as a Karhunen-Loève expansion are not required (see [11, 40]).

The software architecture used here is based on the software component technology and the middleware ‘Component Template Library’ (CTL) [45], which provides an adequate network environment to enable code communication under a prescribed protocol and more generally code coupling. The basic idea of software component technology is to divide a software framework into several tasks and then to implement software components, each of them being able to carry out this particular task. Existing software can be turned into a component by defining an interface through which the communication will be channeled. Implementing a component from a pre-existing program consists in coding a set of methods that other software can call through this interface. In the case of Monte Carlo simulations, two different tasks can be identified. One is to generate a Gibbs process and to transfer this result defining the inclusions geometry in a structured mesh. The other is to run a computation with this given geometry within the mechanical model defined in the first section. Based on the FEM code Feap [77], a CTL software (e.g., see [34, 50, 51]) component named coFeap has been derived [29]. The second component in charge of the geometry generation (the so-called client in Fig. 7) will ask for several runs of the coFeap component at the same time, each of them using a different meso-structure realization.

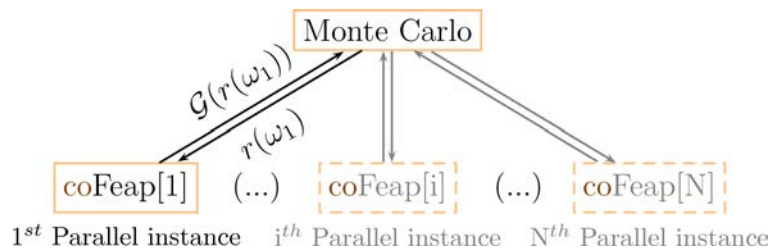


Fig. 7. Parallel software architecture for Monte Carlo simulations using the coFeap component.

Further details on the use of this parallel framework and results are presented in the following Sec. 3.

2.3. Probabilistic characterization of two-phase materials at the macro-scale

At the macro-scale, the major mechanisms which are present at the meso-structure level have to be represented as well. By taking an ‘energetic’ look, one sees that there has to be at least an energy storage functionality for the reversible part of the material behavior – represented through a stored energy function – and an energy dissipating functionality for the mechanically irreversible material behavior, represented through a dissipation function. This corresponds to the description of ‘generalized standard materials’. Here, it is well-known that these functions can act as thermodynamic potentials respectively pseudo-potentials (see e.g., [21, 39, 41, 44]), and are thus sufficient to describe the behavior alluded to.

To achieve a probabilistic description for such a phenomenological model, it is then conceptually sufficient to model these two functions as random variables – or rather random fields to take account of the spatial variation. In this short overview for the extension towards the stochastic situation we will follow the development as outlined in [48, 57–60].

2.3.1. Boundary conditions for the RVE

Let us just for a moment only look at the determination of the elastic constants – assuming linear elasticity and hence a quadratic stored energy function – then it is well known that by just averaging

either the stiffnesses or the compliances, one can derive well-known upper or lower bounds for the said constants. In a situation where one has a separation of scales, one may argue that the RVE is subjected only to constant global strain or stress, as variations of those quantities over the size of the RVE are negligible and will vanish asymptotically.

Hence, the RVE computation to determine the macro-properties may be performed for either Uniform Static Boundary Conditions (USBC), or for Uniform Kinematic Boundary Conditions (UKBC). The results from such computations still form upper or lower bounds respectively, which are better than the well-known averaging ones mentioned earlier, but there may still be a considerable gap [27, 28, 52]. This means that from such a computation with either one of the uniform boundary conditions it is not possible to assign a unique value for the macro-scale constants. This can be seen as an additional uncertainty for the case where one wants to sequentially pre-compute macroscopic properties, which has to be included into the probabilistic description.

This means that – at least for situations with high macroscopic strain or stress gradients – the results from the sequential approach may be at least dubious. This problem with the boundary conditions is unfortunately one of the so-called FE²-method [14]. In such cases with high macroscopic strain or stress gradients, another approach is to actually allow for a finite scale ratio of macro- to meso-scale, and compute macroscopic quantities with the actual global strain field, which does not have to be uniform. This approach is then not sequential any more, and will be described closer in Sec. 3, see also [19, 23, 42, 43].

2.3.2. Macro-scale probabilistic description

On the macro-scale one wants to end up with – disregarding for a moment the probabilistic aspect – a conventional continuum mechanics description [21]. We look at an elasto-plastic material as the simplest instance of a rate-independent description. Rate dependent irreversible mechanisms can be dealt with similarly and are actually mathematically simpler. The elasto-plastic material may serve as a model problem, as other dissipative mechanisms can be formally treated in a completely analogous manner [44].

Coming back to the situation alluded to in the beginning of Subsec. 2.3.1 we look at a quadratic stored energy function [48, 59, 60]. At the beginning it is sufficient to just consider a material point $x \in \mathcal{D}$. Denote the stress tensor by σ_x , the total strain due to some displacement u by $\epsilon_x(u)$, the plastic strain by ϵ_{px} , and the hardening variables by η_x . From these quantities we construct the generalised plastic strain $E_{px} = (0, \epsilon_{px}, \eta_x)$, and the generalised total strain $E_x = (\epsilon_x(u), \epsilon_{px}, \eta_x)$. Herewith, we define the stored energy bilinear form

$$a_x(E_x, E'_x) := (\epsilon_x(u) - \epsilon_{px}) : C_x : (\epsilon'_x(u) - \epsilon'_{px}) + \langle \eta_x, H_x \eta'_x \rangle_x, \quad (8)$$

where C_x is the fourth-order elasticity tensor at x , H_x a hardening modulus, and the bilinear form $\langle \cdot, \cdot \rangle_x$ an appropriate duality pairing depending on the specifics of the hardening variables [48, 59, 60]. From this a Helmholtz free energy may be defined by

$$\psi_x(E_x) := \frac{1}{2} a_x(E_x, E_x). \quad (9)$$

Now if the macro-scale point $x \in \mathcal{D}$ corresponds to some meso-structure ensemble and RVE, all quantities in (8) have to be modelled as random quantities, effectively making the stored energy in (9) a random quantity. It can be shown [48, 59, 60], that a probabilistic plasticity problem at a material point may be formulated with the averaged quantities, i.e., the expected values of those in (8) and (9):

$$a_x(E_x, E'_x) := \mathbb{E}(a_x(E_x, E'_x)). \quad (10)$$

To develop an equation for the whole body, these quantities have to be integrated over the body, i.e., the domain \mathcal{D} , to give the probabilistic bilinear form for the whole body

$$\mathbf{a}(\mathbf{E}, \mathbf{E}') := \int_{\mathcal{D}} \mathbb{E}(a_x(E_x, E'_x)) dx, \quad (11)$$

where the quantities in bold signify fields or functionals on the level of the elasto-plastic body in the domain \mathcal{D} . A completely analogous extension has to be performed for the dissipation functional, see [48, 59, 60]. Having obtained stochastic versions of the Helmholtz free energy and the dissipation function, one ‘only’ has to formally follow the normal derivation of evolution equations for generalized standard materials, to obtain a stochastic version of the elasto-plastic problem with hardening.

With the definition $\mathbf{w} := (\mathbf{u}, \mathbf{E})$ to represent all deformation-like random fields, such that the random strain field \mathbf{E} corresponds to the random displacement field \mathbf{u} , and setting $\mathbf{a}(\mathbf{w}, \mathbf{w}') := \mathbf{a}(\mathbf{E}, \mathbf{E}')$, as well as – analogous to (11)

$$\langle \mathbf{w}, \mathbf{w}' \rangle_P := \int_{\mathcal{D}} \mathbb{E}(\mathbf{u}(x) \cdot \mathbf{u}'(x)) + \mathbb{E}(\epsilon_x(u) : \epsilon'_x(u)) + \mathbb{E}(\langle \eta_x, \eta'_x \rangle_x) dx, \quad (12)$$

for the inner product, defining the generalized exterior random force field as $\mathbf{f} = (f, \mathbf{0})$ to match the deformation-like random field \mathbf{u} , as well as dual stress-like quantities $\mathbf{w}^* := (0, \Sigma)$ – with the random fields of generalized stress $\Sigma := (\sigma, \sigma, \theta)$, where σ is the random Cauchy-stress field, and θ is the random field of thermodynamic fluxes corresponding to the hardening – one may finally announce that [48, 59, 60] *there are unique time evolutions $\mathbf{w}(t)$ and $\mathbf{w}^*(t)$ which solve the mixed stochastic elasto-plastic problem*, such that for all \mathbf{z} and for all $\mathbf{z}^* \in \mathcal{K}$

$$\mathbf{a}(\mathbf{w}(t), \mathbf{z}) + \langle \mathbf{w}^*(t), \mathbf{z} \rangle_P = \langle \mathbf{f}(t), \mathbf{z} \rangle_P, \quad (13)$$

$$\langle \dot{\mathbf{w}}(t), \mathbf{z}^* - \mathbf{w}^*(t) \rangle_P \leq 0. \quad (14)$$

Here, the closed convex set \mathcal{K} in the space of generalized random stress fields represents the ‘elastic domain’, the relation (13) represents the stochastic equilibrium equation, and (14) represents the stochastic normal flow rule, and the superimposed dot in (14) is a weak time derivative. The set \mathcal{K} is quite simply the set of all generalized random stress fields $\mathbf{w}^* = (0, \Sigma)$ with $\Sigma = (\sigma, \sigma, \theta)$, such that the random Cauchy-stress field σ_x satisfies a stochastic yield condition almost surely almost everywhere in the body \mathcal{D} . Here, we choose a general quadratic function $\phi_x(\sigma_x) := 1/2(\sigma_x : Y_x : \sigma_x) + \sigma_x : \tau_x + s_x$, the square root of which will serve as a yield function. Here, Y_x is a random field of positive definite fourth order tensors, τ_x is a random field of strain-like quantities to shift the origin of the general quadric $\phi_x(\sigma_x)$, and s_x a scalar random field to determine the yield level. The elastic domain \mathcal{K} is then simply the set of all generalized random stress fields, such that the associated random Cauchy-stress field satisfies $\sqrt{\phi_x(\sigma_x)} \leq \sigma_x^y$ almost surely at almost all $x \in \mathcal{D}$, where σ_x^y is a random field of yield stresses.

To actually compute the solution [48, 59, 60], developments which parallel the stochastic FEM [46, 47] have to be carried out, including a stochastic form of the closest point projection so well-known in computational plasticity. In Fig. 8 one may see an example of such a computation – the example is the well-known Cook’s membrane – where one may see the initial grid, the deformed grid for a deterministic computation with average material parameters, and the average deformation for a fully stochastic computation along Eqs. (13) and (14). For the same example we show in Fig. 9 one of the possible results of such a stochastic computation, here the exceedance probability for a certain level of the shear stress.

With the ability to perform such stochastic computations for inelastic materials, these may now serve as a macro-scale representations for heterogeneous media as explained before. What is needed additionally is the macro-scale identification of random material parameters, which will be sketched out in Subsec. 2.3.4.

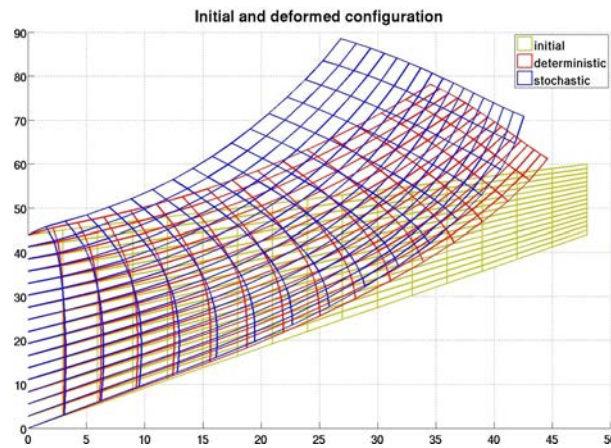


Fig. 8. Deformations for stochastic elasto-plastic model.

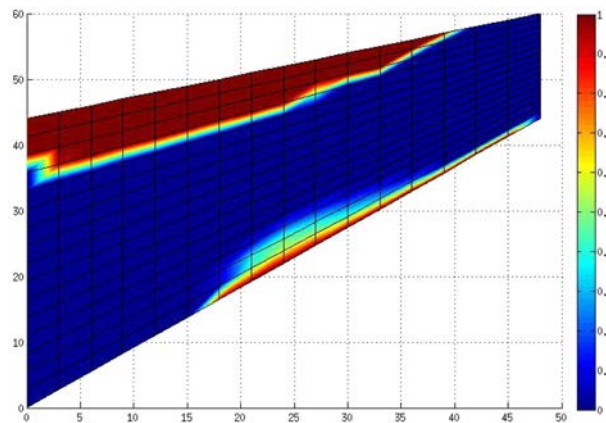


Fig. 9. Exceedance probability of a certain shear stress level.

2.3.3. Probabilistic description of positive definite tensors

A short interlude is necessary to explain one possibility for the probabilistic description of random positive definite tensor fields, such as C_x and H_x which appear in the internal energy bilinear form (8), or the field Y_x used for the elastic domain \mathcal{K} , see also [61, 62]. For positive scalar fields the problem will be described in more detail in Subsec. 2.5.1.

Conceptually, the problem is no different for tensor fields. In Subsec. 2.5.1, the problem is solved by modelling the logarithm of a positive scalar. The final exponentiation then makes everything positive. This may be seen as a simple manifestation of a general principle: the positive numbers are a Lie group under multiplication, which is made into a Riemannian manifold by introducing a metric on the corresponding Lie algebra, the additive group (and vector space) of all real numbers, which is the tangent space at the group identity, the number one. The maps between Lie algebra and Lie group are the exponential and logarithm, respectively. This then has the effect that zero and infinity are both infinitely far away from any finite positive number.

This general prescription is also followed for positive definite tensor fields. These are geometrically an open cone in the space of all symmetric tensor fields [61, 62], and can be given the structure of a Lie group. The corresponding Lie algebra is the vector space of all symmetric tensor fields, and the exponential and logarithm – also defined for the case of symmetric tensors – are again the maps to make the correspondence between the Lie algebra and the Lie group. This again has the effect that singular tensors or tensors with a singular inverse are infinitely far away from any finite positive definite tensor.

2.3.4. Macro-scale properties identification

The probabilistic identification of macroscopic properties to represent the heterogeneous random meso-structure will follow Bayes's rule, which is the preferred way of incorporating information into a stochastic model. In [61, 62] this is described for the case where the identification is performed through measurements – although in that publication the measurements were ‘virtual’ ones. The Bayesian update for a random variable with finite variance boils down to an orthogonal projection. By sacrificing some information gained from the measurement, this can be approximated by a simpler linear update which is reminiscent of the well-known Kalman filter – actually the Kalman filter can be shown [62] to be the low-order part of this new linear update.

In Fig. 10 one may see the probability density functions prior to any identification and after a measurement – the posterior one. Here, we replace the measurement by a meso-structure computation, and the identification proceeds completely in the same manner. What was shown in Fig. 10 for a single parameter (the shear modulus, although, as described in Subsec. 2.3.3 we identify the logarithm of the shear modulus) can be performed for all random fields needed here, i.e., C_x and H_x which appear in the internal energy bilinear form (8) (or rather their logarithms), the (logarithm of the) field Y_x in the yield function, as well as the random fields τ_x , s_x , and σ_x^y in the yield criterion $\phi_x(\sigma_x)$ in Subsec. 2.3.2.

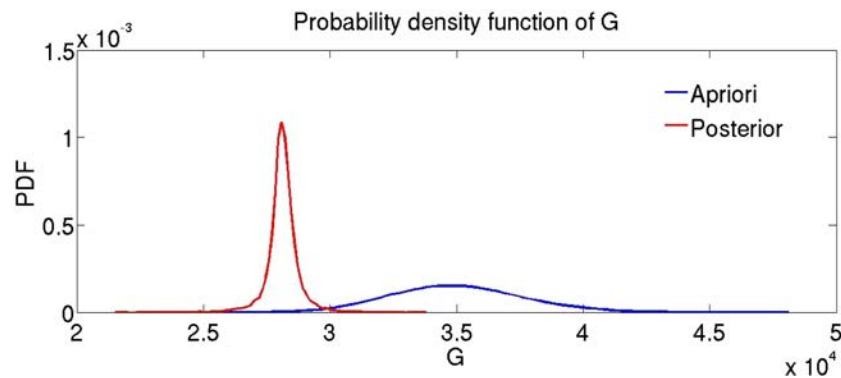


Fig. 10. Prior and posterior for the identification of shear modulus.

2.4. Determination of statistical RVE size

As we have already mentioned in the introduction part, macroscopic models are usually based on the concept of RVE. Here, we focus on the notion of statistical RVE (see [52]) leading to a volume element large enough to assure that its macroscopic properties are assumed to be deterministic, up to a certain tolerance. Obviously, such size strongly depends on the properties to be considered and we restrain our analysis to geometrical properties, namely the void volume fraction. Following [30], the methodology adopted consists in estimating the void volume fraction mean $\bar{\rho}$ and variance σ_ρ^2 along different domain sizes. In order to get those estimates we used the Monte Carlo framework presented before considering a set of 10,000 realizations for each volume fraction and domain size. As a result, Fig. 11 shows the 0.95 confidence interval along the domain size. This confidence interval is defined for one realization as $[\bar{\rho} - 1.96\sigma_\rho; \bar{\rho} + 1.96\sigma_\rho]$.

Table 1 as well as Fig. 11b shows, the SRVE size corresponding to 5% relative error for different voids volume fraction. Clearly the SRVE size is decreasing with an increasing porosity. Typical porosity values for mortars are in the 5% to 10% range and so leading to a 0.07–0.15 m morphological SRVE estimate range. As we mentioned before, although the same methodology might be followed in different cases, this estimate does not provide any information about SRVE size linked to any non-linear mechanical properties (e.g., a macroscopic yield stress).

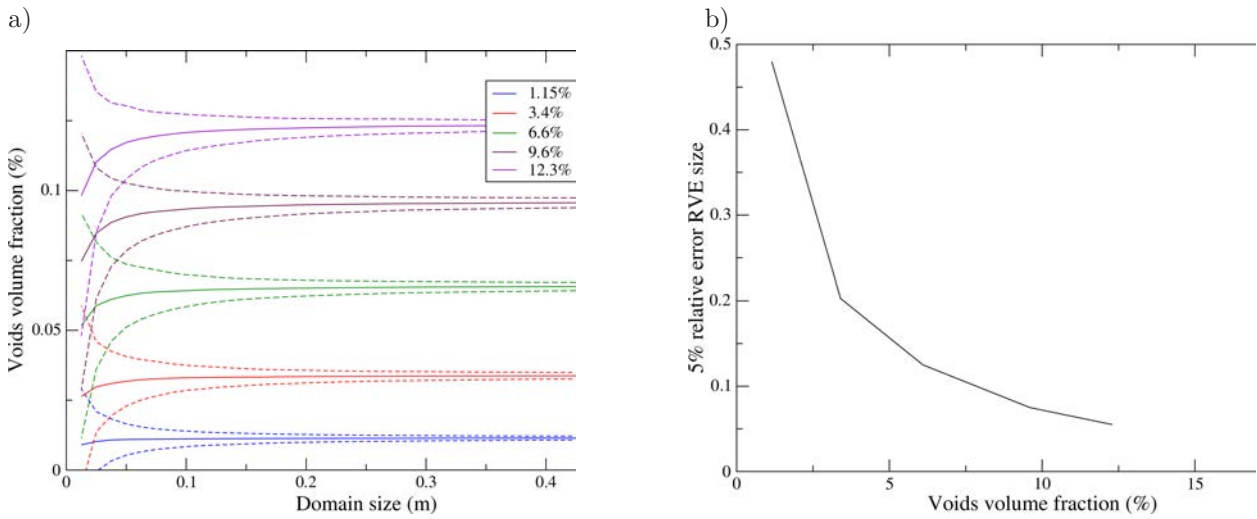


Fig. 11. a) Voids volume fraction confidence interval (0.95) along domain size b) 5% relative error morphological RVE size.

Table 1. SRVE size for different mean voids volume fractions and 5% relative error.

ρ [%]	1.15%	3.4%	6.1%	9.6%	12.3%
SVRE size [m]	0.48	0.203	0.125	0.075	0.055

2.4.1. Simple tension test: numerical results and discussion

By using the stochastic numerical integration method detailed in the previous section, we performed $Z = 10,000$ integration points, each of them corresponding to an independent meso-structure realization. These Monte-Carlo integration points have been distributed on nine processors and we shall present here the different results.

The first point to be mentioned deals with the void volume fraction for each meso-structure geometry. To some extent those data might be viewed as the “input” parameters according to the stochastic integration method. We recall here that each meso-structure realization is built by using a modified Gibbs point process with inclusion radii bounded between 1 mm and 3 mm. Figure 12 shows the void volume fraction (ratio of the void volume versus the total volume) histogram corresponding to the Z realizations. The associated mean value is 6.26% and the standard deviation is 3.59%.

The stochastic integration process is leading to a set of Z axial reaction force-displacement diagrams. Figure 12 shows a subset of 100 realizations. It is worth to recall again that the variability shown by this sample is due only to the meso-structure geometry variability (the material parameters are assumed to be deterministic and so constant along the realizations). Moreover, we shall note that some meso-structures included in this sample have obviously no voids. This point is directly linked to the Gibbs point process features, in particular to the discrete Poisson’s law leading to an inclusion number which is possibly zero.

Figure 13 shows the estimated mean macroscopic stress-strain curve as well as the 99.9% confidence interval. Since this confidence interval is quite narrow the number of integration points for the stochastic integration method is sufficient to make accurate conclusions and to provide good estimates of statistical moments. Moreover, the macroscopic stress σ and strain ε are defined as equivalent homogeneous quantities,

$$\varepsilon = \frac{\bar{u}}{L_x}, \quad \sigma = \frac{\sum_i R_i}{L_y}, \quad (15)$$

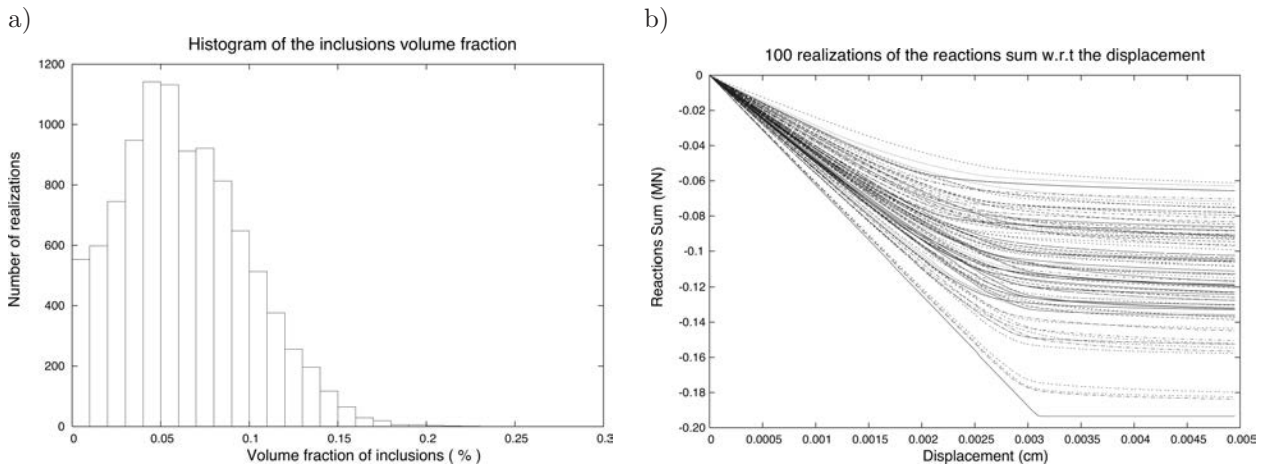


Fig. 12. a) Void volume fraction histogram, b) 100 realizations sample results.

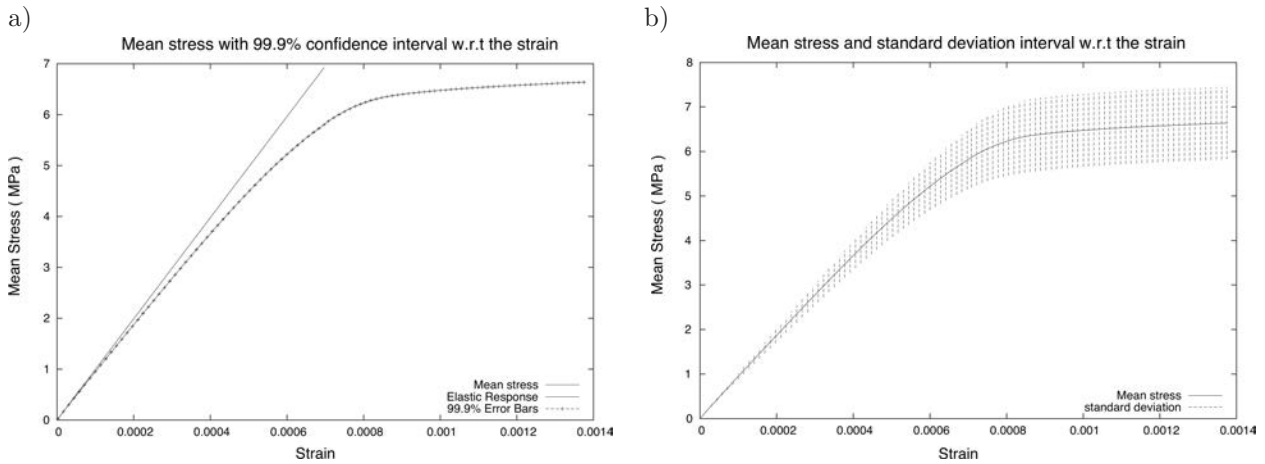


Fig. 13. Macroscopic mean stress w.r.t. the macroscopic strain: a) 0.999 confidence interval, b) standard deviation.

where L_x and L_y are the size of the domain and R_i the axial reactions. This macroscopic mean curve leads to the determination of an estimate for the macroscopic mean Young's modulus as well as to an estimate of the mean maximum stress σ_f . Table 2 summarizes the statistical macroscopic estimates obtained from this numerical example. Those estimates are quite good candidates to be employed in the context of a macroscopic phenomenological model, here for the 1D case. Actually these macro model parameters might be used in order to define macroscopic random fields, and therefore, a stochastic macro-model (that would have to be solved using any stochastic integration method). It is worth to note that the only missing data in order to fully define weakly homogeneous second order random fields is the covariance function. In the simplest case, such second-order information might be given according to one scalar parameter only, the macroscopic correlation length.

Table 2. Statistics of macroscopic quantities.

	Mean Estimator	std-dev interval
σ_u	6.63 MPa	[5.82 MPa, 7.45 MPa]
σ_y	2.49 MPa	[2.15 MPa, 2.54 MPa]
E	9.93 GPa	[9.27 GPa, 10.60 GPa]

2.5. Size effect representation

Size effects for quasi-brittle materials can be experimentally demonstrated at macro-scale and several ways exist of dealing with its modelling. Most of them are linking the micro-cracks coalescence phenomenon which consists in the failure process as a first step to such a size effect [4]. An extensive literature exists on that topic, from the early studies of Weibull (see [73]) dealing with infinite chains built from brittle links (theory of the weakest link), to the current two concurrent theories of Bazant on the one side and of Carpeneri on another. The first one tends to describe the size effect as a deterministic theory of strength redistribution in a Fracture Process Zone (FPZ), the size of which is proportional to a characteristic length, that leads to energetic dissipation. At some level, the micro-cracks' coalescence occurs, and that induces both heterogeneous behavior and some kind of localization, and is strongly intricate to the size effect. Hence, a way to study the fracture of quasi-brittle material is to study the size effect. Recently, Bazant has developed a new theory as a combination of this previous theory with Weibull's one leading to the so called energetic-statistical size effect (see [3]). Another theory combining a non-local model and a stochastic approach has been developed in [63]. On the other hand, Carpeneri's theory is based on the study of quasi-brittle materials seen as materials with a fractal micro-structure (see [10]).

Our goal is to stress the possibility to model the size effect, taking place at the macro-scale, with the use of correlated random fields for macroscopic properties. With some basic assumptions, such macroscopic random fields are in the simplest case characterized by their marginal (point-wise) distributions as well as their spatial mean and covariance function, which of course have to match the first two moments of the marginal distribution. Adding an isotropy condition, this covariance function might be parametrized using, for example, a unique scalar value: the correlation length L_c . This length plays a key role in the context of size effects. Contrary to classical macroscopic models which are based on the RVE concept only, L_c actually defines a scale to which the whole structure size is compared. In that sense, such correlated fields naturally incorporate size effects. Moreover, to some extent such a correlation length L_c might be considered as the "characteristic length" which needs to be defined when using well-known macroscopic non-local models [56]. However, contrary to this characteristic length for which there is a lack of physical interpretation, the correlation length L_c as well as the marginal distribution necessary to characterize random fields for the macroscopic properties might be retrieved from a two-scale analysis like the one presented in the previous section. Thus, we indicate here a complete macroscopic modelling methodology, starting from properties and uncertainties at the meso-scale (which appears to be the most pertinent one considering mechanical failure of cement based materials) up to macroscopic behavior.

As an example of this methodology in a 1D context, we first begin to recall some of the key points dealing with random fields and the Karhunen-Loève expansion, which is one of the most efficient ways of representation in a computational context. Then, we turn to the macroscopic description of the model and its integration using once again direct Monte Carlo simulations.

2.5.1. Random fields for material properties and their Karhunen-Loève expansion

The macroscopic 1D model we consider here represents a three-stage failure process which is typical of cement based materials. After the elastic regime, the inelastic behavior starts through a homogeneous micro-cracking in the so-called Fracture Process Zone (FPZ). Such a phenomenon might be modelled by a volume dissipation process, and phenomenological macro-models are obviously good candidates for this. Once having reached a certain loading limit, the coalescence of the micro-cracks turns to some kind of localization and macro-cracking. For this last stage (and so just before the structure's failure), phenomenological models are no more valid, mainly due to two points: first they are leading to some mesh dependence which is typical of softening laws; second because due to localization the RVE concept is not applicable. To overcome this drawback, many authors have turned to well-known non-local theories which consist in considering a characteristic length. Another way is to consider strong discontinuity models like the one presented in Subsec. 2.1 for the

meso-scale. In the 1D context this model requires four parameters to fully describe all the failure processes (see Fig. 1), namely the elastic modulus E , the yield stress σ_y , the failure stress σ_u and the fracture energy G_f .

In order to model the size effect with such a macro-model, the key idea is to consider its macroscopic parameters (namely σ_y and the gap $e_f = \sigma_u - \sigma_y$) as correlated random fields over the geometric space \mathcal{D} and a probability space Ω . Mathematically speaking, Ω is a space of random elementary events, together with a class of subsets \mathfrak{S} of Ω (*i.e.*, a σ -algebra, see [40]) to which a real number in the interval $[0, 1]$ may be assigned, the probability of occurrence, mathematically a measure P . A \mathcal{V} -valued random variable r is then a function relating to each $\omega \in \Omega$ an element $r(\omega) \in \mathcal{V}$. In case the space \mathcal{V} is a space of functions $\mathcal{F}(\mathcal{D})$ on a spatial domain \mathcal{D} , then r defines a random field. In some sense, this random field r can be viewed as an infinite family of random variables $r(x, \omega)$, assigned at each point $x \in \mathcal{D}$. Both σ_y and e_f are positive and supposed to have a finite known variance. Thus, following the maximum entropy theory (see [65, 69]), these two random variables σ_y and e_f can be taken with lognormal distribution. Without a loss of generality it is convenient to consider that these two random fields are defined as non-linear transformations of two Gaussian random fields γ_1 and γ_2 :

$$\sigma_y = \exp(\gamma_1) \quad \text{and} \quad e_f = \exp(\gamma_2), \quad (16)$$

where γ_1 and γ_2 are fully described by their expected values and their covariances:

$$E\gamma_i(x) \quad \text{and} \quad \text{Cov}_{\gamma_i}(x, y) = V_i \exp\left(-\frac{\|x - y\|}{L_c}\right). \quad (17)$$

In (17) above, we have indicated that the Gaussian random fields γ_1 and γ_2 are supposed to be weakly homogeneous with an exponential form of covariance function and correlation length L_c . As the geometric space is of dimension one, the covariance can be drawn as a surface in a three-dimensional space over the two-dimensional space $\mathcal{D} \times \mathcal{D}$ (see Fig. 14).

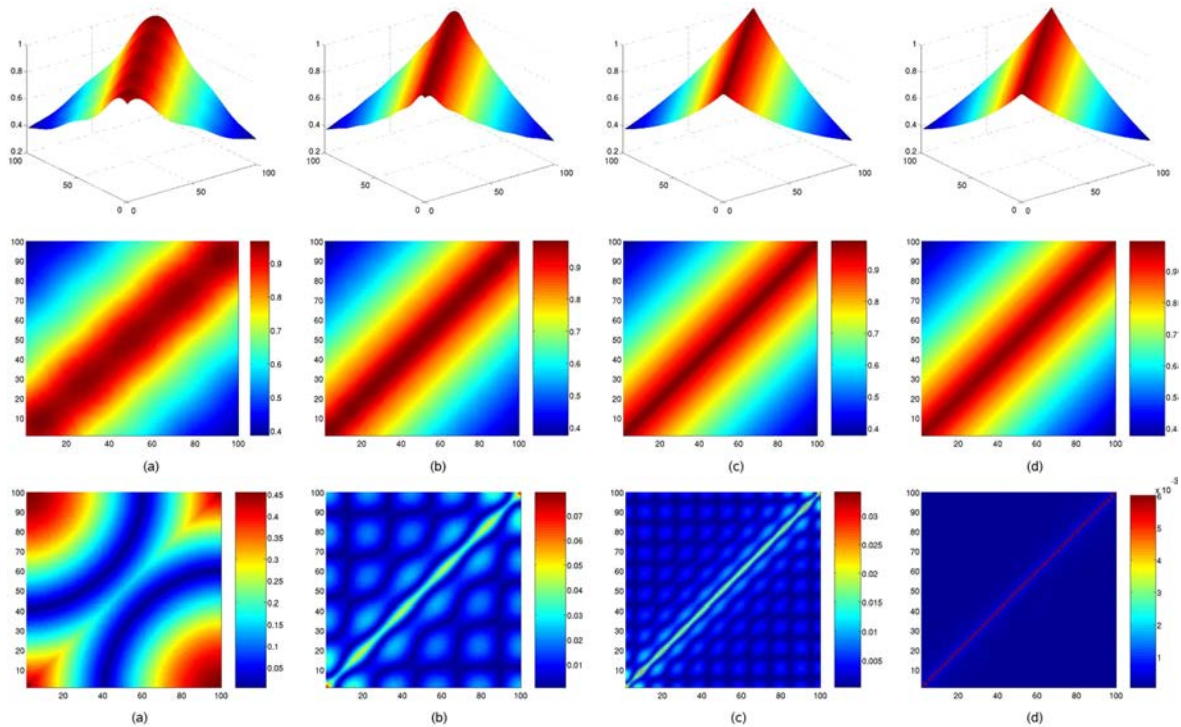


Fig. 14. Random field covariance 3D representation (top row), 2D representation (middle row) and representation error (bottom row), obtained from a) 5, b) 10, c) 20 and d) 50 modes in truncated KLE expansion.

Solving for the response of such a stochastic system essentially consists in computing some response statistics (e.g., its expected value). To that end, we once again employ here the so-called Monte-Carlo method which requires to solve many deterministic systems, each of them being built with realizations $\sigma_y(\cdot, \omega_i)$ and $e_f(\cdot, \omega_i)$ (see Fig. 15) of the random fields σ_y and e_f . In order to provide these realizations an effective computational representation of correlated random fields is needed. One possible way is the Karhunen-Loève expansion (see [40]), which is basically a projection of a given random field onto the eigenvector basis, orthonormal in $L_2(\mathcal{D})$, obtained by the Fredholm eigenvalue problem of the second kind (18),

$$\int_{\mathcal{D}} \text{Cov}_{\gamma}(x, y) \Phi_i(x) dx = \rho_i \Phi_i(y), \quad y \in \mathcal{D}. \quad (18)$$

The solution of this eigenvalue problem for any domain \mathcal{D} is obtained using finite element techniques and provides to a way to synthesize the two Gaussian random fields $\gamma_{i=1,2}$,

$$\gamma(x, y) = \sum_{i=1}^{\infty} \sqrt{\rho_i} \Phi_i(x) \xi_i(\omega), \quad (19)$$

and consequently σ_y and e_f through relations (16). In Eq. (19), the $\xi_i(\omega)$ are uncorrelated Gaussian random variables (with unit variance and zero mean) and thus independent. Having a computational approach in mind, the infinite sum (19) must be truncated. Figure 14 shows the covariance function synthesized using a different number of modes in the KL expansion. These computations have been performed using a modified version of the finite element code FEAP (see [77]).

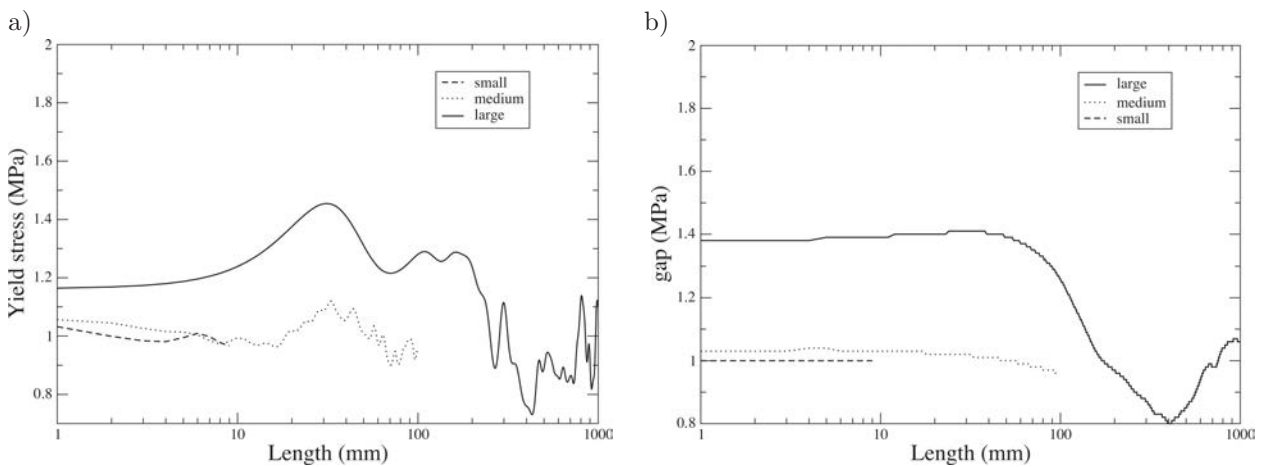


Fig. 15. Normalized realizations of correlated macro random fields σ_y and e_f .

It may be worthwhile to point out that if the correlation function depends only on the distance of the two points, like the one in (17), which is also called stationary, homogeneous, or translation invariant, the computations involved in (18) and (19) can be considerably simplified. This explanation is most easily seen for a simple interval $\mathcal{D} = [0, L]$. Considered in terms of *lags* $x - y$ in (17), the covariance is defined on $[-L, L]$, and since the covariance is even it is a fortiori periodic on this larger interval. Hence embedding the domain \mathcal{D} in a larger one of twice the size, and extending the Fredholm integral equation (18) to this larger domain, one realises that it becomes a convolution equation. As it is well known, this is effectively ‘diagonalized’ by the Fourier transform, turning the convolution into a simple multiplication. This means that the sines and cosines from the Fourier transform – or rather Fourier *series* for the finite interval $[-L, L]$ – are the KL eigenfunctions on this larger interval, and the eigenvalues are simply the corresponding values of the Fourier transform of the correlation function. Hence, one may simulate the process on this larger interval, and then

take as a realisation any subinterval of length L . The transform and the summation in (19) may be performed quickly with the FFT algorithm. Analogous considerations apply in higher dimensions.

2.5.2. Size effect and correlation length

As mentioned before, the 1D macro-model we consider here is based on a strong discontinuity model (see [22]) which leads to the possibility to couple diffuse plasticity or damage (describing the volumetric dissipation due to the homogeneous micro-cracking which takes place in the FPZ) with surface dissipation at the macro cracks. The latter drives the stress to zero without any mesh dependency. Moreover no special precaution has been taken in order to account for the size effect, except considering lognormal correlated random fields for the macroscopic quantities σ_y and e_f .

Considering tensile tests, three different lengths have been treated under displacement control (0.01 m, 0.1 m and 1 m truss), keeping the correlation length equal to $L_c = 0.01$ m. These three cases will be called respectively small, medium and large. It is worth to note that for the medium case, the bar is the same size as the correlation length.

Computing a realization (evaluation of the random field at a given point in the stochastic domain) of γ_1 and γ_2 via the truncated Karhunen-Loève expansion on each of these bars as described previously and using the relations (16) lead to an efficient computational way to represent each realization of the fields σ_y and e_f . The normalized fluctuating part of one realization of σ_y and e_f for each of these bars is shown on Fig. 15. It is worth to note that the larger the bar is in comparison to the correlation length L_c , the more fluctuating the random fields are. Thus, the more likely these macroscopic properties are to have small lower bounds. In terms of strength, such small lower bounds obviously lead to weaker behavior towards failure.

Each of these independent realizations is used to perform Monte Carlo with 10,000 integration points for each case using the coFeap CTL component. Figure 16 presents the cumulative density functions for the maximum load. Considering a given percentile of broken bars, it is worth to note that the smaller the bar is, the higher is its ultimate stress, e.g., 3.68 MPa for the small truss, 3.3 MPa for the medium one, and to 2.87 MPa for the large one. In other words, the strength of the structure is directly linked to its size. The larger is the structure, compared to the correlation length, the weaker it becomes. Moreover, it also has smaller contribution of FPZ in final failure

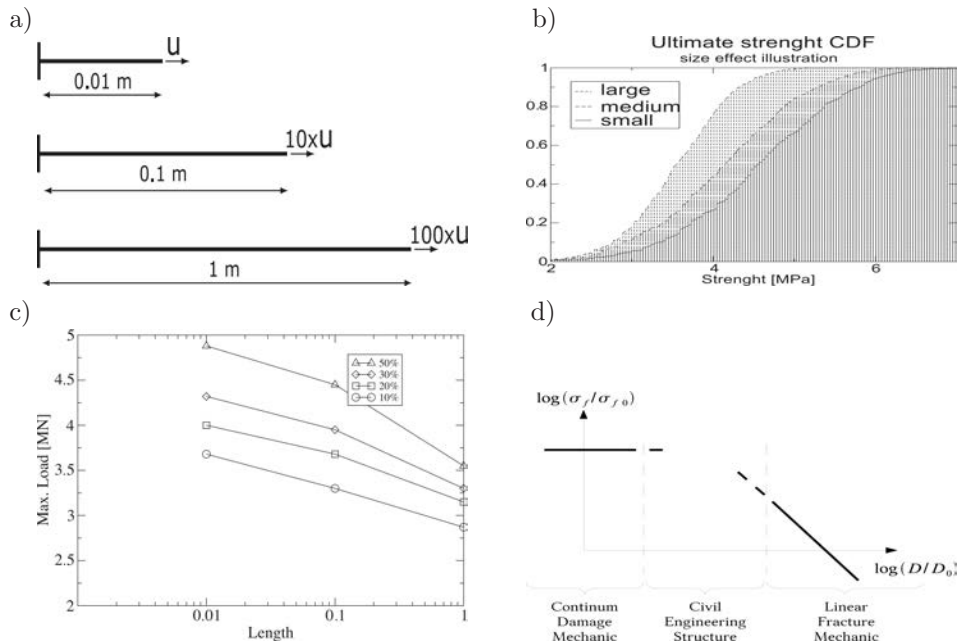


Fig. 16. a) Short, medium and short bar, b) ultimate stress cumulative distribution c) probabilistic size effect diagram, d) standard size effect illustration.

mechanism. Hence, this stochastic way of modelling quasi-brittle failure naturally reveals the size effect. Figure 16 shows the 99% confidence interval with respect to the computations that have been made. For each bar, none of these error bars are overlapping. This point leads to the conclusion that the number of stochastic integration points used for the Monte Carlo process is large enough and thus the results are accurate.

Clearly, the correlation length here plays the key role. Comparable to the characteristic length which appears in the non-local theory, it can be linked to the size of the Fracture Process Zone (FPZ) where micro-cracking occurs. If the size of FPZ prevails relative to the global size of the structure, which is the case for the small bar, the model of Continuum Damage Mechanics (CDM) will well describe the structure's failure and corresponding mechanisms. In the opposite, if the FPZ size is negligible with respect to the size of the structure (i.e., the case of large bar), its influence on the global behavior of the structure is small. Thus, the dominant failure model remains macro-crack that occurs following the model of Linear Fracture Mechanics (LFM).

The modelling procedure for the failure phenomena in quasi-brittle materials proposed herein can be considered as a probability-based attempt to link these two limiting behaviors (LFM and CDM), and provide a sound manner for picking the dominant failure mechanism in each particular case. The likely failure mode for short and (statistically) homogeneous bar pertains to FPZ, whereas the failure mode for long and (statistically) heterogeneous bar is likely a macro-crack. Figure 16 shows that such a kind of size effect interpretation, based upon probability and multiscale providing correlated random fields to describe macroscopic quantities, can provide a sound quantitative description of this important issue in localized failure.

3. SIMULTANEOUS APPROACH TO PROBABILISTIC MULTISCALE ANALYSIS

We see the simultaneous approach is described here not as an alternative, but rather as a complementary and additional method to be used mainly when the sequential approach fails to be applicable. The sequential method may be suspect when the material experiences large strain of stress gradients, or if the pre-computed phenomenological responses on the macro-scale do not cover the material response adequately any more, e.g., when material instabilities, localisation, or cracks start developing.

3.1. Two-scale coupling

A very general mathematical approach for multiscale coupling – but mainly aimed at homogenization – has been described in [1, 13]. One possible approach is to have the meso-scale (or small-scale) evaluation each time a finite element on the macro-scale wants to evaluate a material response, i.e., in each Gauss-point. This has become known as the ‘FE²-method’ [14, 15], and has already been used extensively (e.g., [49, 70–72]). As a Gauss-point has no extension, there is no way in this method to allow for scale-effects – the small scale is assumed to be infinitely smaller than the macro-scale – and hence it is only applicable when there is a really large separation of scales.

Here, we want to allow for the scale effect and do not want to assume a separation of scales. The key idea is to have a finite element on the macro-scale, with displacement field u^M , just be an ‘empty hull’ or window, to be filled with a meso- or small-scale discretisation of displacement field u^m (see Fig. 17). For given values of internal variables ξ^m , the total potential energy can then be written:

$$\Pi^{tot} = \sum_{e=1}^{n_{el}} \left(\underbrace{\int_{\Omega_e^m} \Psi_e(\nabla^s u_e^m, \xi_e^m) d\Omega}_{\Pi_e^{int}(u_e^m)} + \underbrace{\int_{\Gamma_e^m} \lambda_e \cdot (u_e^m - u^M) dS}_{\Pi_e^\lambda(u_e^m, \lambda_e, u^M)} \right) - \underbrace{\int_{\Gamma_N^M} u^M \cdot \bar{t} dS}_{\Pi^{ext}(u^M)}, \quad (20)$$

where $\Psi_e(\nabla^s u_e^m, \xi_e^m)$ is internal energy density, dependent upon micro element displacement and internal variables. The main assumption in (20) is to consider that the internal variables ξ_e^m are only defined at the micro-scale level. For the given value of internal variables, the internal potential energy Π^{int} can be obtained by summing up the contributions in each micro sub-domain e of the internal potential energy of each micro sub-domain Π_e^{int} .

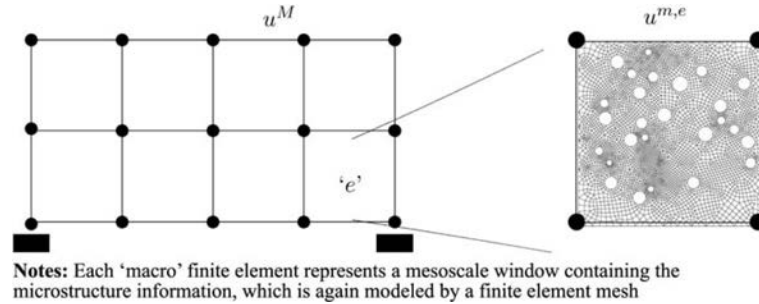


Fig. 17. Macro- and meso-scale finite element model of a simple structure.

Of course now the meshes in adjacent sub-domains do not fit, so the additional term denoted as Π_e^λ , dependent upon the localized Lagrange multipliers λ , is supplied to enforce the correspondence between the micro-scale displacements along the boundary Γ_e^m of each sub-domain and the macro-scale displacements, as suggested in [78] but in a dual form. The coupling term implies an adequate choice of localized Lagrange multipliers and displacement variation. The simplest and most effective method is to just allow linear variations of the displacements along the meso-scale element boundaries [23, 42, 43], along with the Lagrange multipliers reminiscent of hybrid finite elements [21]. We thus obtain [42] a completely analogous element to well-known Pian-Sumihara hybrid stress element [55], but with element arrays representing the corresponding microstructure of heterogeneous material. The inner small-scale mesh is effectively under displacement control, which makes the computations simple and stable. The theory is described in [43], and the computational coupling in [51].

If one wants to allow higher order strain patterns to propagate through the small-scale boundaries, a more elaborate set-up is required. This problem also occurs when structures with different meshes are coupled, and one way to treat this is with localized Lagrange multipliers [53, 54], and this approach has also been adopted here. A similar approach – but not with localized Lagrange multipliers – is the so-called ‘Arlequin-method’ [5, 6], and another multiscale coupling approach may be found in [37, 38]. Our adaptation of the localized Lagrange multiplier method may be found in [18, 19], and a typical meso-model with a discrete – non-continuum mechanics – meso-structure is depicted in Fig. 18, as well as the de-bonding between the phases in Fig. 19, and a macro-crack developing across the macro-element in Fig. 20 in one of the tests computed.

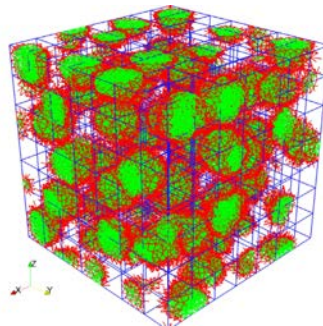


Fig. 18. Meso-scale model.

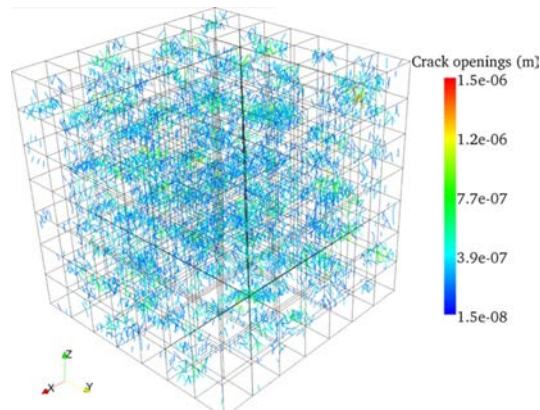


Fig. 19. Meso-scale debonding.

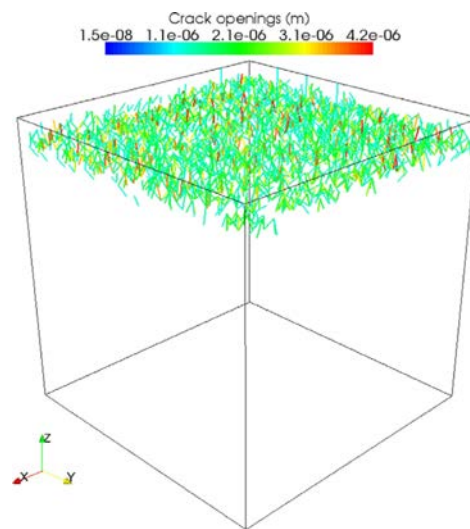


Fig. 20. Macro-scale crack.

3.2. Probabilistic scale coupling

As was already mentioned, both the macro-scale as well as the small-scale are to be considered as uncertain, and hence are modelled in a probabilistic manner. The coupling described in the previous section describes really only the mechanical coupling, but the probabilistic information on both scales has to be coupled as well. It is of course possible to mimic the development of the mechanical coupling, but there is also another possibility, and this is the use of Bayes's theorem. This idea has already been suggested in [36].

We on each scale regard the respective other scale as an essentially 'black box', which we try to approximate with the probabilistic description given on the scale on which we are sitting. It is then quite natural to use conditional expectation to perform the transfer. Conditional expectation corresponds to a projection, and that is what is needed. The difference to what was described in Subsec. 2.5.1, here it is not material properties which are identified, by rather displacements and forces or stresses and strains. Of course a tangent matrix may also be identified if needed in the computational procedure, e.g., in Newton's method.

3.3. Computational coupling

After the mathematics of the coupling has been sketched out, we turn to the code coupling required for the simulation. This was performed with the component framework already mentioned [50, 51]

and [33, 34], which is called ‘Component Template Library’ (CTL), and the computational structure as used in this application is depicted in Fig. 21; it is similar to Fig. 7, only that the Monte Carlo component on top is replaced by the macro-scale component, and the ‘satellites’ at the bottom represent the meso-scale components.

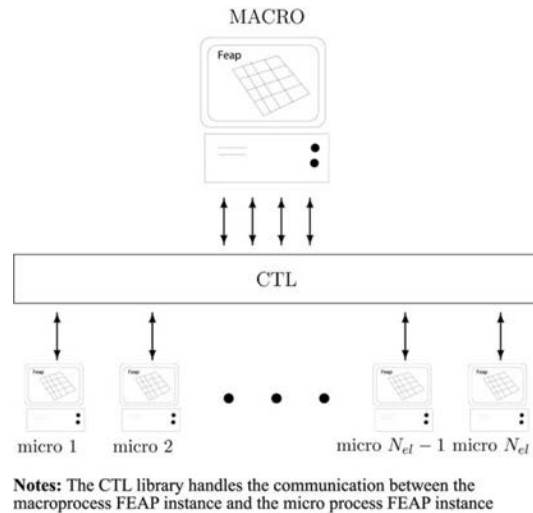


Fig. 21. Task distribution scheme on different processors.

The codes which solve the macro-problem and the ones which solve the small-scale problem may be different, all that is required is that they look like a component. In [43] on each of the scales a version of FEAP (or rather coFEAP) [29, 77] was used, and the small scale just appeared as a new kind of finite element on the macro-scale. This is particularly convenient as all the technology already present in FEAP (like iterative non-linear solvers, etc.) may be continued to use.

In the more elaborate localised Lagrange multiplier framework, FEAP was still used on the small-scale problems, whereas on the large scale a new component (named MuSCAD) was developed for various reasons [18, 19], and a schematic sketch of the computational deployment is shown in Fig. 22. This new component embodied the macro-scale as well as the computations for the coupling via the localised Lagrange multiplier method. On the other hand, it would be perfectly feasible to make the coupling a separate component. This shows the versatility of the component technology [51].

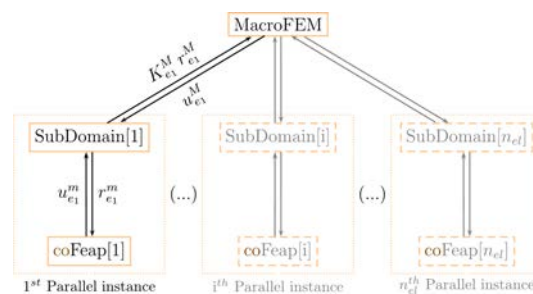


Fig. 22. MuSCAD component interaction in a parallel computation.

Another aspect which can be handled on a coarse-grained basis by the component framework is parallelisation. From Fig. 21 one may easily glean that each component – using its own resources – may run concurrently with all the other components, while all the necessary synchronisation due to the information being passed around is being taken care of by the CTL [50, 51]. Each component may be a parallel code on its own, and also use a parallel processor in these coupled computations. This may be regarded as a fine-grained parallelization, so that we have a multiscale

parallel computation to execute the multiscale mechanical problem, a curious duplicity granting us with significant increase of computational efficiency.

4. CONCLUDING REMARKS

This work provides much improved approach with respect to currently dominant computational strategy for dealing with localized failure of engineering structures, by using phenomenological macro-models with parameters estimated by homogenization. The improvements concern both the model capability to correctly represent failure mechanisms and their subsequent evolution, along with their variability for real-life, heterogeneous materials.

In order to improve predictive modelling of failure when accounting for material heterogeneities, the meso-scale has been here chosen as the one being pertinent to describe failure mechanisms of cement-based composite materials (concrete, mortar etc.). At this scale, the cement-based composites are properly interpreted as heterogeneous, and represented as such by using a special structured mesh methodology granting us computational efficiency. Any such structured mesh relies on a regular grid where elements are not constrained to the physical interfaces between the different phases and can also contain phase interface. For any element crossed by phase interface, as shown here in detail for the classical CST elements, we explained how to enhance the elements kinematics accordingly by using the incompatible modes method providing two kind of discontinuities. The first discontinuity consists in a strain discontinuity inside the element in order to model different elastic properties of the two phases, whereas the second one corresponds to a displacement jump that allows to model the interface failure (e.g., debonding). Such a representation provides much higher computational efficiency than the exact, non-structured mesh adapted to the phase interface. Moreover, the structured element mesh with incompatible modes is more robust than the corresponding X-FEM representation, for it keeps all the extra computations pertinent to phase interface local (or element-wise). Finally, the proposed mesh is also the most suitable for probability computations, since it does not require any remeshing or changing the number of elements for handling different realizations of elements crossed by the phase interface.

Besides such an efficient tool for probability studies, the key idea suggested here to ensure the success of probability computations pertains to identifying the source of uncertainty and providing the corresponding description. In the chosen context of cement-based materials, the variability of the geometric description at the meso-scale level (placing the aggregates within the cement matrix) is the main source of uncertainty. By considering such geometric uncertainty of cement-based materials, we recover the corresponding probability distribution of macroscopic mechanical properties, such as mechanical strength that remains strongly dependent upon volume fraction. Here, for representing uncertainties in meso-scale geometry, we have employed modified Gibbs points processes with circular voids inside a perfectly-plastic Drucker-Prager matrix. Although the material properties of the two phases are assumed to be deterministic, such geometric variability leads to a stochastic problem to be solved at the structural scale with random fields replacing deterministic values of material properties.

Finally, with the macroscopic properties (e.g., yield stress, ultimate strength) described by random fields of this kind and their covariance function (namely the correlation length), we showed that the proposed macro-model provides a very sound interpretation of the size effect. Such size effects are a major issue in modelling quasi-brittle failure like cement-based one and bridge two limit cases of failure, continuum damage mechanic and linear fracture mechanics. The main finding is that the proposed multiscale strategy defining the random field distributions of failure parameters can provide quantitative estimates of dominant failure mode, between the FPZ of continuum damage mechanics for (statistically) homogeneous structure versus the macro-crack of linear fracture mechanics for (statistically) heterogeneous structure.

Another key ingredient of our model granting it predictive capabilities pertains to its ability to accommodate both failure mechanisms, FPZ and macro-crack introducing the displacement

discontinuity and localized failure, and to take into account their interaction. The model thus represents the proper generalization of weakest link from the classical Weibull's theory, which allows it to provide natural explanation of the size effect in structural failure. We note in passing that the model can also recover the classical Weibull's results, simply by considering uncorrelated random field.

We note that many ingredients we employed in probability computations are indeed quite classical, such as KLE representation of random fields, and the Monte-Carlo method to compute the statistical moments of the desired quantities, which would allow us to quickly integrate this approach with other multiscale methodologies. We also note that the use of the Components Template Library (CTL) to provide the multiscale version of the finite elements code FEAP and the subsequent multiscale probabilistic strategy, can be quickly implemented in many other computer codes.

ACKNOWLEDGEMENTS

This work was supported by the French Ministry of Research, and French-German University Fund. An early stage of this collaborative work was supported by Humboldt Research Award and PROCOPE program of French-German collaboration.

REFERENCES

- [1] A. Abdulle, A. Nonnenmacher. *A short and versatile finite element multiscale code for homogenization problems*. Comput. Meth. Appl. Mech. Engrg., **198**: 2839–2859, 2009.
- [2] K.-J. Bathe. *Finite Element Procedures*. Prentice Hall, 1996.
- [3] Z.P. Bažant. *Probability distribution of energetic-statistical size effect in quasibrittle fracture*. Prob. Eng. Mech., **19**: 307–319, 2004.
- [4] Z.P. Bažant, L. Cedolin. *Stability of Structures: Elastic, Inelastic, Fracture and Damage Theories*. Oxford University Press, 1991.
- [5] H. Ben Dhia. *Multiscale mechanics problems: Arlequin method*. Comptes Rendus Academie Sciences, **326**: 899–904, 1998.
- [6] H. Ben Dhia, G. Rateau. *The Arlequin method as a flexible engineering design tool*. Int. J. Numer. Meth. Engng., **62**: 1442–1462, 2005.
- [7] M. Bornert, T. Bretheau, P. Gilormini. *Homogization in mechanics of materials*. Hermes-Science, Paris, 2001 (in French).
- [8] C.A. Canflisch. *Monte Carlo and quasi-Monte Carlo Methods*. Acta Numerica, **7**: 1–49, 1998.
- [9] D. Brancherie, A. Ibrahimbegovic. *Novel anisotropic continuum-damage model representing localized failure. Part I: Theoretical formulation and numerical implementation*. Engineering Computations, **26**(1–2): 100–127, 2009.
- [10] A. Carpenteri. *On the mechanics of quasi-brittle materials with a fractal microstructure*. Eng. Frac. Mech., **70**: 2321–2349, 2003.
- [11] J.B. Colliat, M. Hautefeuille, A. Ibrahimbegovic, H. Matthies, *Stochastic Approach to quasi-brittle failure and size effect*, Comptes Rend. Académie Science: Mech. (CRAS), **335**: 430–435, 2007.
- [12] S. Dolarevic, A. Ibrahimbegovic. *A modified three-surface elasto-plastic cap model and its numerical implementation*. Computers and Structures, **85**: 419–430, 2007.
- [13] W. E, B. Engquist. *The heterogeneous multiscale methods*. Comm. Math. Sci., vol. 1, pp. 87–133, 2003; *preprint as: arXiv:physics/0205048v2 [physics.comp-ph]*, 2002.
- [14] F. Feyel. *Multiscale FE^2 elastoviscoplastic analysis of composite structures*. Comput. Mat. Sci., **16**: 344–354, 1999.
- [15] F. Feyel, J.-L. Chaboche. *FE^2 multiscale approach for modelling the elastoviscoplastic behaviour of long fibre SiC/Ti composite materials*, Comput. Meth. Appl. Mech. Engrg., **183**: 309–330, 2000.
- [16] P. Gilormini. *A shortcoming of the classical non-linear extension of the self-consistent model*. Comptes Rend. Académie Science, **320**(116): 115–122, 1995.
- [17] M. Hautefeuille, S. Melnyk, J.-B. Colliat, A. Ibrahimbegovic. *Failure model for heterogeneous structures using structured meshes and accounting for probability aspects*. Engineering Computations, **26**(1–2): 166–184, 2009.
- [18] M. Hautefeuille, J.-B. Colliat, A. Ibrahimbegović, H.G. Matthies. *Multiscale Zoom Capabilities for Damage Assessment in Structures*, in: *Damage Assessment and Reconstruction after Natural Desasters and Previous Military Activities*. A. Ibrahimbegovic and M. Zlatar [Eds.], NATO-ARW series, Springer, 2008.
- [19] M. Hautefeuille, J.-B. Colliat, A. Ibrahimbegović, H.G. Matthies, P. Villon, *A multi-scale approach to model localized failure with softening*. Computers and Structures, **94–95**: 83–95, 2012.

- [20] A. Hillerborg, M. Mod er, P.E. Petersson. *Analysis of crack formation and crack growth in concrete by means of fracture mechanics and finite elements*. Cement and Concrete Research, **6**: 773–782, 1978.
- [21] A. Ibrahimbegovic. *Nonlinear Solid Mechanics: Theoretical Formulations and Finite Element Solution Methods*. Springer, Berlin, 2009.
- [22] A. Ibrahimbegovic, D. Brancherie. *Combined hardening and softening constitutive model of plasticity: precursor to shear slip line failure*. Comp. Mechanics, **31**: 88–100, 2003.
- [23] A. Ibrahimbegovic, D. Markovic. *Strong coupling methods in multiphase and multiscale modeling of inelastic behavior of heterogeneous structures*. Comp. Meth. Appl. Mech. Eng., **192**: 3089–3107, 2003.
- [24] A. Ibrahimbegovic, S. Melnyk. *Embedded discontinuity finite element method for modeling of localized failure in heterogeneous materials with structured mesh: an alternative to extended finite element method*. Comp. Mechanics, **40**: 149–155, 2007.
- [25] A. Ibrahimbegovic, E.L. Wilson. *A modified method of incompatible modes*. Communications in Applied Numerical Methods, **7**: 187–194, 1991.
- [26] E.T. Jaynes. *Probability Theory: the logic of science*. Cambridge University Press, 2003.
- [27] M. Jiang, M. Ostoja-Starzewski, I. Jasiuk. *Scale-dependent bounds on effective elastoplastic response random composites*. J. Mech. Phys. Solids, **49**: 655–673, 2001.
- [28] M. Jiang, I. Jasiuk, M. Ostoja-Starzewski. *Apparent elastic and elastoplastic behaviour of periodic composites*. Int. J. Solids Struct., **39**: 199–212, 2002.
- [29] C. Kassiatis, M. Hautefeuille. *coFeap’s Manual*. LMT-Cachan Internal Report, **2**: 2008.
- [30] T. Kanit, S. Forest, I. Galliet, V. Mounoury, D. Jeulin. *Determination of the size of the representative volume element for random composites: statistical and numerical approach*. Int. J. Solid Struct., **40**: 3647–3679, 2003.
- [31] M.G. Kendall. *On The Reconciliation Of Theories Of Probability*. Biometrika, **36**: 101–116, 1949.
- [32] M. Kleiber, H. Antunez, T.D. Hien, P. Kowalczyk. *Parameter Sensitivity in Nonlinear Mechanics*. Wiley, 1997.
- [33] M. Krosche, R. Niekamp, H.G. Matthies. *PLATON: A Problem Solving Environment for computational Steering of Evolutionary Optimisation on the Grid*, in: *Proc. Int. Conf. on Evolutionary Methods for Design, Optimisation, and Control with Application to Industrial Problems (EUROGEN 2003)*. G. Bugeda, J.A. D s d ri, J. Periaux, M. Schoenauer and G. Winter [Eds.], CIMNE, 2003.
- [34] M. Krosche, H.G. Matthies. *Component-Based Software Realisations of Monte Carlo and Stochastic Galerkin Methods*. Proc. Appl. Math. and Mech. (PAMM), **8**: 10765–10766, 2008.
- [35] A. Kucerova, D. Brancherie, A. Ibrahimbegovic, J. Zeman, Z. Bitnar. *Novel anisotropic continuum-damage model representing localized failure. Part II: Identification from tests under heterogeneous test fields*. Engineering Computations, **26**(1–2): 128–144, 2009.
- [36] P.-S. Koutsourelakis, E. Bilionis. *Scalable Bayesian reduced-order models for high-dimensional multiscale dynamical systems*. arXiv: 1001.2753v2 [stat.ML], 2010.
- [37] P. Ladeveze, O. Loiseau, D. Dureisseix. *A micro-macro and parallel computational strategy for highly heterogeneous structures*. Int. J. Numer. Meth. Eng., **52**: 121–138, 2001.
- [38] P. Ladev ze, A. Nouy. *On a multiscale computational strategy with time and space homogenization for structural mechanics*. Comput. Meth. Appl. Mech. Engrg., **192**: 3061–3087, 2003.
- [39] J. Lemaitre, J.L. Chaboche. *Mechanics of Solid Materials*. Dunod, Paris, 1988 (in French).
- [40] M. Lo ve. *Probability Theory – Fourth Edition*. **1**: 1977.
- [41] J. Lubliner. *Plasticity Theory*. Macmillan, New York, NY, 1990.
- [42] D. Markovic, A. Ibrahimbegovic. *On micro-macro interface conditions for micro-scale based fem for inelastic behavior of heterogeneous material*. Comput. Meth. Appl. Mech. Engrg., **193**: 5503–5523, 2004.
- [43] D. Markovi . R. Niekamp, A. Ibrahimbegovic, H.G. Matthies, R.L. Taylor. *Multi-scale modelling of heterogeneous structures with inelastic constitutive behaviour: Part I – Physical and mathematical aspects*, Engineering computations, **22**: 664–683, 2005.
- [44] H.G. Matthies. *Computation of constitutive response*, in: *Nonlinear Computational Mechanics – State of the Art*. P. Wriggers and W. Wagner [Eds.], Springer, 1991.
- [45] H.G. Matthies, R. Niekamp, J. Steindorf. *Algorithms for strong coupling procedures*. Comput. Meth. Appl. Mech. Engrg., **195**(17–18): 2028–2049, 2006.
- [46] H.G. Matthies. *Quantifying uncertainty: modern computational representation of probability and applications*, in: *Extreme Man-Made and Natural Hazards in Dynamic of Structures*, A. Ibrahimbegovic and I. Kozar [Eds.], 2007.
- [47] H.G. Matthies. *Stochastic Finite Elements: Computational Approaches to Stochastic Partial Differential Equations*. Zeitschrift f r Angewandte Mathematik und Mechanik (ZAMM), **88**: 849–873, 2008.
- [48] H.G. Matthies, B. Rosi . *Inelastic Media under Uncertainty: Stochastic Models and Computational Approaches*, in: *IUTAM Symposium on Theoretical, Computational, and Modelling Aspects of Inelastic Media*. B.D. Reddy [Ed.], IUTAM Bookseries. Springer, 2008.
- [49] C. Miehe, A. Koch. *Computational micro-to-macro transitions of discretized microstructures undergoing small strains*. Arch. Appl. Mech., **72**: 300–317, 2002.
- [50] R. Niekamp, H.G. Matthies. *CTL: a C++ Communication Template Library*. GAMM Jahreshauptversammlung in Dresden, 21–27 March 2004.

- [51] R. Niekamp, D. Markovič, A. Ibrahimbegovic, H.G. Matthies, R.L. Taylor. *Multi-scale modelling of heterogeneous structures with inelastic constitutive behaviour: Part II – Software coupling implementation aspects*. Engineering computations, **26**: 6–28, 2009.
- [52] M. Ostoja-Starzewski. *Material spatial randomness: from statistical to representative volume element*. Probabilistic Engineering Mechanics, **21**: 112–132, 2006.
- [53] K.C. Park, C.A. Felippa. *A variational principle for the formulation of partitioned structural systems*. Int. J. Numer. Meth. Engng., **47**: 395–418, 2000.
- [54] K.C. Park, C.A. Felippa, G. Rebel. *A simple algorithm for localized construction of non-matching structural interfaces*. Int. J. Numer. Meth. Engng., **53**: 2117–2142, 2002.
- [55] T.H.H. Pian, K. Sumihara. *Rational approach for assumed stress finite elements*. Int. J. Numer. Meth. Engng., **20**: 1638–1685, 1984.
- [56] G. Pijaudier-Cabot, Z.P. Bažant. *Nonlocal Damage theory*. J. Eng. Mech., **113**: 1512–1533, 1987.
- [57] B. Rosić, H.G. Matthies. *Computational Approaches to Inelastic Media with Uncertain Parameters*. J. Serbian Soc. Computational Mech., **2**: 28–43, 2008.
- [58] B. Rosić, H.G. Matthies, M. Živković, A. Ibrahimbegovic. *Formulation and Computational Application of Inelastic Media with Uncertain Parameters*, in: *Proceedings of the Xth Conferrence on Computational Plasticity (COMPLAS)*. E. Oñate, D.R.J. Owen and B. Suárez [Eds.], CIMNE, 2009.
- [59] B. Rosić, H.G. Matthies. *Plasticity described by uncertain parameters – a variational inequality approach*, in: *Proceedings of the XIth Conferrence on Computational Plasticity (COMPLAS)*. E. Oñate, D.R.J. Owen, D. Perić and B. Suárez [Eds.], pp. 385–395, CIMNE, 2011.
- [60] B.V. Rosić, H.G. Matthies. *Stochastic Galerkin Method for the Elastoplasticity Problem*, in: *Recent Developments and Innovative Applications in Computational Mechanics*. D. Müller-Hoppe, S. Löhner and Stephanie Reese [Eds.], pp. 303–310, Springer, 2011.
- [61] B.V. Rosić, A. Kučerová, J. Sýkora, O. Pajonk, A. Litvinenko, H.G. Matthies. *Parameter Identification in a Probabilistic Setting*. arXiv: 1201.4049v1 [cs.NA], 2011.
- [62] B.V. Rosić, A. Litvinenko, O. Pajonk, H.G. Matthies. *Sampling-free linear Bayesian update of polynomial chaos representations*. J. Comp. Phys., **231**: 5761–5787, 2012.
- [63] K. Sab, I. Lalaai. *Unified approach to size effect of quasi-brittle materials*. Comptes Rendus Academie Sciences, **316**: 9, 1187–1192, 1993 (in French).
- [64] E. Sanchez-Palencia. *Introduction to asymptotic methods and homogenization. Application to continuum mechanics*. Hermes, 1992 (in French).
- [65] C.E. Shannon. *A mathematical theory of communication*. Bell System Technical Journal, **27**: 379–423 and 623–656, 1948.
- [66] J.C. Simo, J. Oliver, F. Armero. *An analysis of strong discontinuity induced by strain softening solution in rate independent solids*. Comp. Mechanics, **12**: 277–296, 1993.
- [67] J.C. Simo, R.L. Taylor. *Consistent tangent operators for rate-independent elastoplasticity*. Comput. Meth. Appl. Mech. Engrg., **48**: 101–118, 1985.
- [68] S.A. Smolyak. *Quadrature and interpolation formulas for tensor products of certain classes of function*. Soviet Mathematics Dokl., **4**: 240–243, 1963.
- [69] C. Soize. *Maximum entropy approach for modeling random uncertainties in transient elastodynamics*. J. Acoust. Soc. Am., **109**(5): 1979–1996, 2001.
- [70] I. Temizer, T.I. Zohdi. *A numerical method for homogenization in non-linear elasticity*. Comput. Mech., **40**: 281–298, 2007.
- [71] I. Temizer, P. Wriggers. *On the computation of the macroscopic tangent for multiscale volumetric homogenization problems*. Comput. Meth. Appl. Mech. Engrg., **198**: 495–510, 2008.
- [72] I. Temizer, P. Wriggers. *An adaptive multiscale resolution strategy for the finite deformation analysis of micro-heterogeneous structures*. Comput. Meth. Appl. Mech. Engrg., **200**: 2639–2661, 2011.
- [73] W. Weibull. *A Statistical Distribution Function of Wide Applicability*. J. Appl. Mech., 293–297, 1951.
- [74] E.L. Wilson, R.L. Taylor, W.P. Doherty, J. Ghaboussi. *Incompatible displacement models*. Numerical and Computer Methods in Structural Mechanics, 43–57, Academic Press, New York, 1973.
- [75] E.L. Wilson. *The static condensation algorithm*. Int. J. Num. Meth. Eng., **8**: 199–203, 1974.
- [76] I.O. Yaman, N. Hearn, H.M. Aktan. *Active and non-active porosity in concrete. Part I: Experimental evidence*. Materials and Structures, **15**: 102–109, 2002.
- [77] O.C. Zienkiewicz, R.L. Taylor. *The Finite Element Method, 6th edition, Volumes 1 and 2*, Elsevier, Oxford, 2005.
- [78] T.I. Zohdi, P. Wriggers, C. Huet. *A method of substructuring large-scale computational micromechanical problems*. Comput. Meth. Appl. Mech. Engrg., **190**: 5639–5656, 2001.
- [79] T.I. Zohdi, P. Wriggers. *Introduction to Computational Micromechanics*. Springer, 2005.